INVISCID MODELING OF AIRCRAFT TRAILING VORTICES

Vernon J. Rossow

Ames Research Center

SUMMARY

A survey is presented of inviscid theoretical methods that have proven useful in the study of lift–generated vortices.   Concepts derived using these inviscid theories are then presented which have helped to guide research directed at alleviating the velocities and rolling moments imposed on aircraft entering these wakes.

INTRODUCTION

The purpose of this conference is to present a status report on research directed at reducing the disturbances to the air behind aircraft as they fly through the atmosphere.   The objective of such a reduction is to minimize the hazard to smaller aircraft that might encounter these wakes.   The general guidelines given this research are that natural atmospheric motions be assumed negligible so that the alleviation schemes will be effective on calm days when the wakes are believed to be most persistent.   A further restriction is that the alleviation is to be achieved by aerodynamic means, hopefully to be accomplished by changes on the wake–generating aircraft that are easy to retrofit onto existing aircraft.

With these guidelines as a background, this paper first presents an overview of inviscid theoretical methods that have been found useful in the study of lift–generated wakes.   Several wake–alleviation schemes developed by use of inviscid theory are then described.   The effect of viscosity and turbulence on these theories is discussed only briefly to indicate the limits of applicability of some of the methods because a survey of theoretical methods that include viscosity and turbulence is the subject of the next paper.   The reader is directed to references 1–8 for other papers that review

9

and summarize research on vortices from a historical or technical point of view not restricted to alleviation.

NOMENCLATURE

$\mathbb{R}$. aspect ratio

b span of wing

C_L lift coefficient, $\dfrac{\text{lift}}{(1/2)\rho U_\infty^2 S}$

     local lift coefficient

C_l rolling-moment coefficient, $\dfrac{\text{rolling moment}}{(1/2)\rho U_\infty^2 Sb}$

c wing chord

$\bar{c}$ mean geometric chord

$f(\Gamma_o/\nu)$ Iversen's Reynolds number function

$\ell(y)$ local lift

N number of vortices

r radius of vortex

S wing area

T dimensionless time $= \dfrac{4t\Gamma_o}{b^2}$

t time

U_∞ free-stream velocity; alined with x axis

V_1 maximum circumferential velocity in vortex

v_θ circumferential velocity in vortex

X,Y,Z	dimensionless coordinates, for example, $X = \dfrac{2x}{b}$
x,y,z	coordinates, x is streamwise and z is vertical
a	angle of attack
Γ	circulation
γ	circulation in point vortices
ν	kinematic viscosity
ρ	air density

Subscripts

f	following model that encounters wake
g	model that generates wake
o	centerline value of circulation
v	vortex

OVERVIEW OF FLOW FIELD

It is conyenient to divide the flow field into the several regions indicated in figure 1. The rollup region lies immediately behind the wake-generating aircraft where the wake character is changing rapidly with distance. because of self-induced distortions. The plateau region is that axial incre-ment of the wake where the vortices have a nearly constant structure. The decay region includes that part wherein substantial diffusion of vorticity occurs due to viscous and turbulence effects. Various vortex dispersion mechanisms such as vortex instabilities, bursting, or breakdown can occur in any of these three regions and their character may or may not depend on viscosity and turbulence. The boundaries of these regions are determined experimentally.

Since the wake is produced by the lead or wake-generating aircraft, any analysis of the lift-generated wake begins with and depends on the completeness and accuracy of the description of the flow field around the generator aircraft. This aspect of the wake-vortex problem has received considerable attention during the past several decades, but a general method is not yet available for finding the complete flow field in order to precisely define the initial conditions for the wake. However, very good approximations to the lift-distribution and wake-starting conditions may be obtained by use of inviscid vortex-lattice computer programs. The status of these methods can be found in references 9 to 12. Efforts are currently being made to include the effect of the rollup of the wake on the lift distribution (e.g., refs. 12-15). The comparisons in figure 2 (prepared by Maskew using the method of refs. 13 and 14) show that the rollup of the vortex sheet can affect the span loading substantially at the wing tips when the wing is at high angles of attack. The agreement of that prediction with the experimental span-loading measurements of Chigier and Corsiglia (ref. 16) is much better than the result obtained when the vortex wake is assumed to remain flat or in a plane without rolling up from its edges. Such a change in span loading has an effect on total lift, but the much larger effect appears in the distribution of vorticity in the wake. Caution should therefore be exercised when a flat wake is assumed in calculating the span loading on the generating wing because the loading gradients at the wing tip may not represent the correct concentration of vorticity. Most of the wind-tunnel studies at Ames Research Center were made at small angles of attack (i.e., $a \lesssim 12°$) so the accuracy of the flat wake approximation was adequate. For these calculations, a modified version of a program by Hough (ref. 17) was used.

Downstream of the generating aircraft, the vorticity shed by the lifting surfaces usually rolls up into two or more counterrotating (or pairs) vortices in the rollup region shown in figure 1. This process is approximated quite well by inviscid analyses, but as the wake ages (i.e., further downstream) viscosity and turbulence cause differences to increase between the inviscid result and the actual flow field. Flow processes that occur in the so-called rollup and plateau regions (discussed later) may be approximated

12

fairly well by inviscid theories, but the decay region requires more complete theories that include viscosity and turbulence.

The wake-vortex problem exists because, at some distance behind the generating aircraft, another aircraft may encounter the wake. The objective of this research program is to first evaluate the loads caused by the wake on this following aircraft and then to reduce them to a tolerable level by some sort of alleviation scheme. Although many types of encounter are possible, the NASA program concentrated on the axial penetration of the wake (indicated in fig. 1) because it seemed the most likely to happen during landing. The flow field over the follower induced by the wake is then approximated by the same inviscid steady-state theories used to model the generator, but an allowance must now be made for the nonuniform properties of the incoming airstream. Another section describes the theories used to analyze the flow over the follower and the comparisons made with experiment.

WAKE ROLLUP

Several methods are discussed here for predicting how the vorticity distribution in the wake immediately behind the lift-generating surfaces changes from a nearly flat spanwise distribution into two circular regions of vorticity (fig. 3). This reshaping process is usually referred to as the rollup of the wake or vortex sheet shed by the wing. The methods and topics discussed now are:

- Two-dimensional time-dependent motion of point vortices
- Three-dimensional time-dependent motion of vortex filaments
- Direct- and inverse-rollup theories
- Plateau and decay regions for isolated vortex

Ideally, it would be desirable to treat the rollup of the distributed vorticity by a numerical scheme that includes the boundary layer on the wing, fuselage, and other surfaces along with the drag of the landing gear and the

thrust of the engines. Finite–difference methods for the two– and three–dimensional time–dependent aspects of the flow field are being developed and improved upon by several research groups with the hope that such a more complete analysis of the wake can be made. Although these more complex methods make it possible to more accurately represent the structure of the wake, they are not easy to use and require variable grid sizes and larger amounts of computer time. Since these methods usually include viscosity, they will not be discussed further here. Methods specifically designed for reducing wake velocities are discussed in another section.

Two–Dimensional Time–Dependent Motion of Point Vortices

Since the velocity field of a point vortex is known in closed form, a simple representation of the wake is obtained by replacing the continuous distribution of vorticity with a distribution of point vortices that move with time. This method was applied to vortex sheets by Rosenhead (ref. 18) and Westwater (ref. 19) over 40 years ago and it has been used extensively since then to estimate the reshaping of the vorticity distribution in wakes with time or distance behind the generating wing. The analysis is carried out as a two–dimensional time–dependent problem in the so–called Trefftz plane (fig. 3). An example of an elliptically loaded wing is presented in figure 4 (taken from ref. 20). Estimating the wake restructuring by such a time–dependent method has two principal difficulties. The first is to assess the numerical accuracy of the calculations and the second is to interpret the results.

A variety of papers have elaborated on the shortcomings of the method and have introduced ways to remedy these shortcomings (e.g., refs. 21 to 27). These discussions generally agree that the spiral shape at the edges of vortex sheets is often not well simulated by the vortex array and that the point vortices sometimes undergo excursions believed to be associated with the vortex array and not with the vortex sheet being represented. Several methods have been introduced recently (refs. 25 to 27) to stabilize these vortex motions and to eliminate the excursions believed not to be a part of the vortex–sheet structure. Although these techniques suppress vortex excursions

and sheet kinking, they also introduce another error source. The use of finite cores in the vortices suggested by Chorin **and** Bernard (ref. 25) and Kuwahara and Takami (ref. 26) or the accumulation of vortices at the center of the spiral as suggested by Moore (ref. **27**) all contain arbitrary parameters not related to the conservation equations for the fluid they are to represent. The computed results may then appear more reasonable than those obtained from point vortices, but the quantitative accuracy is uncertain. Finite vortex cores instead of point vortices were used in some of the cases analyzed, and the vortex motions were smoothed. The qualitative nature of the solutions was found not to change if the core radius chosen for the vortices was less than the initial spacing of the vortices. However, the vortex motions were found to depend on the core size chosen. Another method has recently been introduced by Maskew (ref. 14) which enables an improved representation of continuous vortex sheets by breaking the primary discrete vortices used in the representation into subvortices when and where needed.

Numerical accuracy - The motion of a number of two-dimensional point vortices in an incompressible fluid is a problem for which numerical calculations are known to be unstable; consequently, any initial error grows with each time step. Fbr this reason, the calculations are usually begun with a large number of significant figures (double precision on most computers) in the hope that the desired result can be achieved before accumulated errors wipe out all the accuracy. It is also essential that the accuracy or error accumulation be monitored during the calculafions to detect an inappropriate choice of mesh size or excessive error growth. For example, Westwater (ref. 19) used the first moment of vorticity as an indicator of accuracy. When suitable error monitors are used, it is possible to determine whether seemingly unrealistic results are attributable to numerical error or to properties of the vortex array being analyzed.

Three error monitoring parameters are used in the calculations made at Ames:

(1)   The first moment of vorticity for each side (to reduce the likeli-
hood of compensating errors due to symmetry):

$$\bar{y}\Gamma_o = \bar{y} \sum_{j=1}^{N/2} \gamma_j = \sum_{j=1}^{N/2} y_j \gamma_j \tag{1}$$

(2)   The second moment of vorticity **J**   about the center of gravity for
the vortices on each side:

$$J = \sum_{j=1}^{N/2} \left[\left(y_j - \bar{y}\right)^2 + \left(z_j - \bar{z}\right)^2 \right] \gamma_j \tag{2}$$

(3)   The Kirchhoff–Routh path function   Wr   for the entire array of
vortices (e.g., ref. 28):

$$Wr = \sum_{i=1}^{N-1} \sum_{j=i+1}^{N} \left(\frac{\gamma_i \gamma_j}{4\pi}\right) \ln \left[\left(y_i - y_j\right)^2 + \left(z_i - z_j\right)^2 \right] \tag{3}$$

Note that none of these quantities are used in the time–dependent calculations
nor do they depend on the numerical integration scheme used.   They are period-
ically evaluated (usually after every 10 or 20 steps) to ascertain how much
error has accumulated in the positions of the assembly of vortices.   **It** was
found that the Kirchhoff–Routh path function was the first to indicate the
presence of errors in the calculat'ions and that the first moment of vorticity
was hardly ever affected; that is, the first moment is the least sensitive of
the three accuracy monitors.   When enough significant figures are retained
in the results to cover the plotting accuracy, the gross aspects and trends
of the vortex sheet observed in various experiments appear to be modeled
correctly.

Interpretation of *data* – The interpretation of the point vortex distribu-
tion in terms of a continuous distribution is not straightforward.   A tech-
nique from reference 20 provided a vortex structure when a group of point
vortices in the wake were known to be associated with a given rotational
motion, for example, vortices on one side of an elliptically loaded wing.

Within each such group, the distribution of point vortices was first reinterpreted as a stepwise radial distribution of circulation about the centroid of vorticity for one side of the wing. This was done by assuming that the vorticity associated with a point vortex in the array is spread uniformly on a ring with a radius equal to the distance of the vortex from the centroid. As indicated in figure 5, the resulting stepwise curve for circulation as a function of radius agrees quite well with the variation predicted by Betz' theory (refs. 29 and 30) for elliptic loading even though rollup is not entirely completed (fig. 4(b)). A faired curve through the stepwise variation could then be used to determine the circumferential velocity distribution in the vortex.

An interpretation difficulty does not arise, however, in those situations wherein the observation point lies well outside the vortical region. For example, representation of the wakes of most conventional aircraft in the far field by two point or line vortices is quite adequate for determining their motion in the presence of the ground and a crosswind. Comparisons of theoretical positions measured for vortices (e.g., refs. 31–35) and a predicted unsteady pressure field with that measured on the ground (ref. 36) provide insight into the adequacy of the approximations for various circumstances.

Three-Dimensional Time-Dependent Motion of Vortex Filaments

The point vortex representation of quasi-two-dimensional wakes can be extended into the full three-dimensional time-dependent case by use of vortex filaments instead of point vortices. Typical applications of this technique to the analysis of wake vortices has been made in references 37 to 44. Summation of the contributions to the velocity field (e.g., by the Biot-Savart law) must be made along the entire length of each filament rather than just a pointwise summation. The increase in calculation time required becomes cumbersome and introduces further sources for numerical errors and instabilities. Unfortunately, simple conservation relationships are not available for three-dimensional filaments that permit an easy evaluation of error growth as the computation proceeds. A further complication not present in the two-dimensional case is that infinite self-induced velocities occur if the

filament is assumed to have zero core radius. This difficulty is usually circumvented by assuming an artificial core or cutoff radius within which the velocity decreases to zero as the center of the filament is approached. The numerical solution therefore may or may not depend strongly on the core radius or axial flow along the core (e.g., ref. *44).* If the solution is strongly dependent on core diameter, the analysis should probably be carried out by use of a finite–difference method so that a more realistic representation of the vorticity distribution is used in the theoretical model.

Despite the foregoing disadvantages, the vortex–filament approximation has been useful in predicting the more general structure of aircraft wakes as they approach airports. Considerable effort has also been devoted to the investigation of the self–induced instabilities of a vortex pair observed by Scorer (refs. *45, 46)* and others to sometimes be responsible for the breakup of aircraft wakes (e.g., refs. *45–48).* The initiation and growth characteristics of these instabilities (which can lead to breakoff and linking to form loops from two parallel and counterrotating vortices) are reviewed in the section on inviscid alleviation schemes.

Direct– and Inverse–Rollup Theories

Direct–rollup theory – A theoretical tool frequently used to study the circumferential velocity distribution in lift–generated vortices is the simple rollup method of Betz (ref. 29). His theory is based on the conservation equations for inviscid, two–dimensional vortices and relates the circulation in the fully developed vortex to the span loading on the generating wing. The simplicity of the method results from the assumptions that the vortex is completely rolled up and that the rollup process is inviscid. To achieve a unique result, the vortex sheet is assumed to roll up in an orderly fashion from the wing tip inboard, so that successive layers of the sheet are wrapped around the center and over previous wrappings (fig. **3**). Any axial or stream–wise variation in the flow velocity is assumed to have a negligible effect on the rollup process. The Betz method does not treat the transition or intermediate stages between the initial vortex sheet behind the wing and the final rolled–up vortex structure. When the derivation is completed

(e.g., ref. 30), the vortex structure is related to the span loading on the generating wing by

$$\Gamma_v(r_1) = \Gamma_w(y_1) \tag{4}$$

where the radius in the vortex r_1 is related to a spanwise station on the wing y_1 by

$$r_1 = -\frac{1}{\Gamma_w(y_1)} \int_{b/2}^{y_1} \Gamma_w(y)\,dy \tag{5}$$

The symbol Γ_w denotes the bound circulation on the wing and Γ_v, the circulation in the fully developed vortex. Although the Betz theory does not appear to have been used extensively for a number of years after its first derivation, it has recently been demonstrated by Donaldson et al. (refs. 49, 50) to be useful and often more accurate than more complex methods. The favorable publicity given to the Betz method by Donaldson led to an elaboration of the theory and the more examples by Mason and Marchman (ref. 51) and to the use of the rollup theory by Brown (ref. 52) to predict the axial flow velocity in the vortex. A typical example of the good representation provided by the inviscid rollup theory is presented in figure 6. The experimental data (ref. 53) were obtained with a three-component hot-wire probe, and the span loading for the Betz calculation was obtained with a vortex-lattice theory (ref. 17). It appears that viscous effects have not altered the vortex structure appreciably in these cases. Recently, Bilanin and Donaldson (ref. 54) have extended the rollup theory to include the drag of the wing and of turbulence injection devices.

Inverse rollup theory - As more experimental velocity data were accumulated with the ground-based facilities (refs. 53 and 55), it became desirable to relate the vortex structure backward to the span loading on the wing that generated the vortex. This led to what might be called an inverse-Betz method (ref. 56) based on the same basic equations and assumptions as the direct-Betz method. The derivation is begun with the expression presented previously that relates the radius r_1 in the vortex to the spanwise

19

station on the wing y_1 which contains a given amount of circulation. After some simple manipulations and because the vortex is axially symmetric, so that the circulation may be written as $\Gamma_V = 2\pi r_1 v_\theta$, the inverse relationship becomes

$$\frac{b}{2} - y_1 = r_1 + \int_0^{r_1} \frac{d(rv_\theta)}{v_\theta} \tag{6}$$

where v_θ is the measured circumferential velocity in the vortex.

Two sample cases presented in figures 7(a) and (b) include the measured vortex structure, the span loading inferred from these measurements by the inverse rollup method, and, for comparison, the span loading predicted by vortex–lattice theory. These results show that the inverse rollup theory can recover the span loading on the generating wing fairly accurately. With almost all configurations, a difference occurs near the wing tip as a result of the finite core size and solid–body rotation in the vortex near $r = 0$. The magnitude of the distortion in span loading depends on the size of the core, which is influenced by the character of the boundary layer on the wing and on the viscous and turbulent shear forces in the vortex itself. In most cases, these distortions appear to be small and to occur only near the wing tip.

Region of applicability of rollup theories - The simplicity of both the direct and the inverse rollup methods results from the assumptions that the vortex is completely rolled up and that the rollup process is inviscid. These two assumptions then limit the downstream interval over which the theories apply. The upstream end of the region of applicability begins where the rollup of the vortex sheet is largely completed and can be estimated by use of inviscid, time–dependent rollup calculations. Results such as those in figures 6 and 10 of Rossow (ref. 20) indicate that a major part of the rollup process behind many wings can be considered practically complete within as few as 3 to 5 span lengths behind the generating wing.

The downstream end of the region of applicability is the distance at which viscous and turbulent decay of the vortex has modified its structure to the extent that the inviscid theory no longer approximates it. An

20

estimate for this limit can be obtained from the recent data of Ciffone and Orloff (ref. 55) wherein a so-called plateau region (discussed in the next section) is identified. Within this plateau region, they found that the vortex decays very little, but it is followed by a region where the vortex decays roughly as $t^{-1/2}$. These considerations suggest that the region of applicability of the Betz method lies between about 3 span lengths and the downstream end of the plateau region, which is estimated from the data of Ciffone and Orloff (ref. 55). Another consequence of the inviscid rollup assumption is that excessively high velocities are often predicted at and near the center of the vortex. Nevertheless, comparisons made by Donaldson et al. (refs. 49, 50, and *54)* have shown that outside the core region (radius of maximum circumferential velocity), the Betz rollup theory yields reliable estimates for the vortex structure.

Plateau and Decay Regions for Isolated Vortex

The accuracy with which both the inviscid direct- and inverse-Betz methods relate the span loading to the vortex structure suggests that either the early history of the vortex is nearly inviscid or that the decay process is very slow. The correct interpretation appeared when the circumferential velocity was measured by Ciffone and Orloff (ref. 55) at a number of stations behind several generating wings. Figure 8, taken directly from their paper, shows that the maximum circumferential velocity is essentially unchanged for approximately *40* span lengths behind those three wings. The expected decay of the vortex, which is inversely proportional to the square root of distance, then begins to occur. The two straight lines for each configuration shown in figure 8 approximate the data in each region. The presence of both a plateau (nearly inviscid) and a decay region is also indicated in Donaldson's analysis (ref. 57) of the decay of a vortex using his second-order closure model for turbulence. Since a wide variety of wing planforms all exhibited the same characteristic plateau and decay regions, Iversen (ref. 58) set about finding an explanation for the onset of decay. By using a self-similar turbulent vortex, he was able to correlate the data obtained in ground-based facilities and in flight into the single curve shown in figure 9 (taken from Iversen, ref. 58).

Iversen's Reynolds number function $f(\Gamma_0/\nu)$ is conveniently equal to 1.0 for Reynolds numbers over 10^6. From the data of reference 55 and these correlation functions, Ciffone (ref. 59) has developed an empirical relation—ship that makes it possible to predict easily the end of the plateau region and the peak swirl velocity in vortices. The information gained by Iversen (ref. 58) and Ciffone (ref. 59) was then extended by Iversen (ref. 60) to a numerical analysis of an isolated vortex using a mixing length model for the eddy viscosity. The initial data for the structure of the vortex were obtained using the rollup theory based on span loading. The numerical analy—sis is then able to predict the structure of the vortex in the plateau region, through the transition process, and into the decay region.

The simple Betz rollup theories assumed that each vortex in the pair acts independently of the other (i.e., as if it were isolated). The fact that such an assumption is valid for large distances into the wake was predicted in the theoretical work of Nielsen and Schwind (ref. 2, p. 413). The very slow decay of an isolated vortex or of a single pair indicates that radical changes must be made in these lift—generated wakes if the hazard to encountering aircraft is to be substantially reduced.

ROLLING MOMENT ON ENCOUNTERING WING — AXIAL PENETRATION

Another aspect of the wake—vortex problem that is approximated fairly well by inviscid theory 'is the estimation of the rolling moment on a wing as it encounters the wake vortices. A simple and reasonably accurate method is needed to not only evaluate the rolling—moment hazard posed by wakes of exist—ing aircraft but also to compare alleviation schemes. The NASA studies were restricted to axial penetrations and cross—vortex penetrations were not studied. (Refs. 1, 2, 5, 53, and 61-88 present the results of studies of the wake encounter problem.) This is not meant to imply that a cross—vortex encounter is less hazardous, but that entry into the vortex along the axis is probably the most likely to occur during landing and takeoff operations. If the flight path of the following aircraft is along or only slightly off axial, the flow field is approximated by steady—state theories. The schematic diagram in figure 10 indicates the way in which the rolling moment on the

following wing is analyzed. The axial or streamwise velocity is assumed equal to the free-stream velocity. The vertical components of the circumferential velocities in the vortices are used as the upwash or downwash on the follower wing by adding the contributions of the one or more pairs of vortices in the wake. The torque on the following wing is then reduced to coefficient form by

$$C_{l_f} = \frac{\text{rolling moment}}{(1/2)\rho U_\infty^2 S_f b_f}$$

In the study at Ames reported in reference 53, the torque or rolling moment on the encountering wing was calculated by

1. Two-dimensional strip theory
2. Strip theory with empirical lift-curve slope correction
3. Vortex-lattice theory; flat-wake approximation

The two-dimensional strip theory for the rolling moment assumes that the lift on each spanwise wing element is given by its two-dimensional value or

$$l(y) = C_{L_a} \sin a \, \tfrac{1}{2} \rho U_\infty^2 c(y) \tag{7}$$

where C_{L_α} is the two-dimensional lift-curve slope of the airfoil section at that spanwise station, $\sin a \approx w/U_\infty$ is the flow inclination, and $c(y)$ is the local chord of the wing. When the quantity $y l(y)$ is integrated across the span of the rectangular wings used in reference 53, the rolling-moment coefficient becomes (e.g., refs. 20 and 53)

$$C_{l_f} = \frac{C_{L_\alpha}}{b_f^2} \int_{-b_f/2}^{b_f/2} (w/U_\infty) y \, dy \tag{8}$$

The values presented in table I were found by integrating equation (8) numerically after setting w/U_∞ equal to the sum of the measured v_θ/U_∞ contributions of the left- and right-hand vortices. A different form of equation (7) can be obtained when only one vortex is acting on the following wing by setting $w/U_\infty = v_\theta/U_\infty = \Gamma(r)/2\pi r U_\infty$ and with $y = r$:

$$c_{l_f} = 2 \left(\frac{C_{L_\alpha}}{2\pi} \right) \left(\frac{b_g}{b_f} \right)^2 \int_o^{b_f/2b_g} \left[\frac{\Gamma(r)}{b_g U_\infty} \right] d\left(\frac{r}{b_g} \right) \tag{9}$$

Although equation (9) is sometimes more convenient, equation (8) is used here because it is believed to be more accurate for the wakes being considered.

For two-dimensional wings, the lift-curve slope, C_{L_a}, is usually taken as 2π. As noted in table I (reproduced from ref. 53), the predictions made with $C_{L_a} = 2\pi$ are then generally too high because it does not account for the induced angles of attack near the wing tips and near the vortex centerline. An empirical relationship for the lift-curve slope to be used in the calculation of torque may be obtained by use of the formula introduced by R. T. Jones (p. 95 of ref. 89):

$$C_{L_\alpha} = \frac{2\pi \mathbb{R}}{P \cdot \mathbb{R} + 2} \tag{10}$$

where $\mathbb{R}$ is the aspect ratio and P is semiperimeter/span. Maskew* compared the rolling moment calculated by vortex-lattice theory and by the strip theory with several versions of equation (10). He concluded that the span, aspect ratio, and perimeter in equation (10) should be interpreted on the basis of half a wing when the vortex and wing center are aligned. He reasoned that each half wing then acts as a separate wing, and equation (10) should be interpreted accordingly. For the rectangular wings studied here, equation (10) then becomes

$$C_{L_\alpha} = \frac{2\pi \mathbb{R}_f}{\mathbb{R}_f + 6} \tag{11}$$

The strip-theory predictions corrected for C_{L_α} by equation (11) are noted in table I to be in good agreement with the vortex-lattice theory and in fair agreement with experiment. The vortex-lattice theory used is a version of

_____

*B. Maskew, Hawker Siddeley Aviation, Ltd. (NRC Associate at Ames Research Center), private communication.

24

Hough's (ref. 17) and of Maskew's (ref. 13) methods adapted to the present situations. The differences that occur between the vortex–lattice theory and experiment may be due to any of the following: differences in the interpretation of the measured rolling moments; differences in the vortex velocity data (e.g., large axial velocities), a combination of both, or unsteady aspects of the wind–tunnel measurements due to meander of the vortex which were assumed negligible. Nevertheless, the foregoing results indicate that either the vortex–lattice theory or the simple strip theory with C_{L_a} determined by the Jones–Maskew formula provides reasonable estimates for the rolling moment induced by a vortex on a follower wing.

With the empirically adjusted strip theory, the rolling moment and lift on a wing can be simply calculated at a large number of points in the wake. Contours of equal rolling–moment coefficient and lift interpolated from these points are presented in figure 11 for one vortex and one span ratio. Only one quadrant is presented because the flow field is symmetrical vertically and antisymmetrical about the centerplane. Although the contours are not as precise as if determined by vortex–lattice theory, they do indicate the nature of the area over which high values of rolling moment occur. As expected, the maximum rolling moment occurs when the encountering wing is centered approximately on the vortex. Aircraft typically have the control capability to create a rolling–moment coefficient of *0.04* to 0.06 *so* that any imposed torque by a vortex that causes C_{l_f} to exceed about 0.06 will cause the encountering aircraft to roll even when full counterroll control is imposed. The shaded area in figure 11(a) within the contour labeled 0.06 can then be interpreted, for example, as a hazardous region where overpowering rolling moments are to be found. Similarly, the results in figure 11(b) indicate that large values of positive and negative lift are induced on the follower by the vortex wake, depending on its location relative to the vortex pair. As expected, the shapes of the curves of constant torque and lift change with both the vortex structure and with the span of the follower. The dependence of the rolling moment on distance behind the generating aircraft are not discussed because downstream changes in the structure of a two–vortex developed wake depend largely on viscosity and turbulence.

25

ALLEVIATION SCHEMES BASED ON INVISCID THEORY

Past research has shown that the wakes of conventional lifting systems on aircraft persist as a single vortex pair for unacceptable distances behind the generating wing. The slow rate at which vorticity is dispersed from such a single pair suggests that changes must be made in the flow field of the generating wing so that the wake is tolerable when it is fully developed. Therefore, the topics to be treated here are:

- Centroid of vorticity consideration
- Span loading for large vortex cores
- Sawtooth loadings for vortex dispersion
- Self-induced vortex excursions
- Convective merging of vortex cores

The alleviation schemes discussed in these subsections are based on modification of the flow over the generator to produce certain flow mechanisms in the near wake which disperse the lift-generated circulation. The first subsection describes one approach for selecting desirable characteristics in the span loading for alleviation. Several conceptual vortex wakes that have been useful in guiding our wake-vortex minimization program are then presented along with some of their characteristics. Although the guidelines presented are still being developed, they serve to indicate a direction for research and to identify desirable features in the flow field that could provide alleviation.

Centroid of Vorticity Consideration

Since the span loading on the generating wing goes to zero at both wing tips, the wake contains equal amounts of positive and negative vorticity. If the loading falls off monotonically from a maximum at the centerline to zero at the wing tips, the wake rolls up into one vortex per side or a single pair. Although the net circulation in the wake is zero, considerable . distance or time behind the generating wing is required (to mix on a two-dimensional basis) before the two concentrations of opposite vorticity combine or diffuse enough to have, in effect, a vanishing circulation

throughout the wake. One way to shorten the distance for complete mixing of circulation is to decrease the effective span by making the net shed circulation zero over a smaller part of the span. One obvious point for such a subdivision is at the wing centerline. The effectiveness of such a consideration is demonstrated by first considering the conservation of the first moment of circulation and the relationship between span loading and shed vorticity. By inviscid theory, the spanwise location of the centroid of vorticity $\bar{y}$ shed by the lifting surface remains fixed for each side of the wing. Hence, far behind the wing, the centroid of shed vorticity is located at the same spanwise station as at the wing, which is given by

$$\bar{y} = \frac{-1}{\Gamma_{C_L}} \int_0^{b_g/2} y \, \frac{d\Gamma(y)}{dy} \, dy = \frac{1}{\Gamma_{C_L}} \int_0^{b_g/2} \Gamma(y) dy$$

where $\Gamma(y)$ is the bound circulation on the wing and Γ_{C_L} is the centerline circulation or the final total circulation in each vortex of the pair far downstream (i.e., $\Gamma)_{x=\infty}$). Since the spanwise loading is related to the bound circulation by

$$\ell(y) = \frac{1}{2} \rho U_\infty^2 c C_\ell(y) = -\rho U_\infty \Gamma(y)$$

the spacing between the vortices in the final pair far downstream is then

$$\frac{b_g'}{b_g} = \frac{C_{L_g}}{[cC_\ell(0)/\bar{c}]} \tag{12}$$

independent of the shape of the span loading used to obtain the lift. Since the strength of the final vortices for a given lift is proportional to $(b_g')^{-1}$, the separation between the vortices, the corresponding circulation is

$$\Gamma)_{x=\infty} = \Gamma_{C_L} = \frac{-\text{lift}}{\rho U_\infty b_g'} = \frac{-cU_\infty C_\ell(0)}{2} \tag{13}$$

On the basis of these simple considerations, final weak or low-intensity vortices are therefore obtained by reducing the lift at the wing root or aircraft centerline as much as possible while C_{L_g} is held fixed. Such a

27

possibility has been demonstrated in the data obtained by Ciffone (ref. 90) behind a model of a Boeing 747 in a water tow tank with dye flow visualization. Measured distances between vortices far downstream yielded values for four flap configurations as b_g'/b_g = 1.03, 1.25, 1.50, and 1.72. On the basis of these measurements, the circulation in the final vortex is reduced to 1.03/1.72 (or 60%) by the one flap configuration that has 30 percent of its inboard end cut off as compared with the conventional landing configuration — a substantial reduction. Both configurations shed the same number of vortices, but the latter has a better balance between positive and negative circulation for wake alleviation. Confirmation of the reduced circulation in these cases by measuring the velocity or rolling moment in the wake has not been made. Theoretical span loadings (fig. 12) for the wing alone without a fuselage as centerbody indicate that the far-field separation between the vortices would be $b_g'/b_g \big)_{theory}$ = 1.22, 1.26, 1.28, and 1.31. Although the order of magnitude of these predicted results is about right, the disagreement between 1.31 and 1.72 is not small. The differences in the configurations used in the theory and experiment probably account for some of the differences in the predicted and measured values of b_g'/b_g. Also, some merging of vortices may still be in progress at the farthest downstream station observed.

Other theoretical separation distances can be found by subdividing the span loading differently to approximate different vortex interactions. However, more theoretical and experimental information is needed to guide the theory and the interpretation of the vortex separation distances. The subsections that follow therefore present some mechanisms by which vortices merge or combine and some guidelines for promoting, enhancing, or preventing the merger. This discussion is not concerned with the lifting efficiency or any drag penalty of the alleviation schemes, but the first objective is to determine what can be done. When promising configurations are identified, it will then be necessary to optimize the alleviation concept by including more complete considerations of the entire aircraft.

Span Loadings for Large Vortex Cores

A variety of wing shapes have been considered experimentally and theoretically as a means to reduce the high circumferential velocity in

lift-generated vortices. These configurations were studied because it was thought that enlarging the vortex core would reduce the swirl velocity and the rolling moment associated with a given lift. The direct relationship between span loading and vortex structure provided by the Betz rollup theory suggested that wing planform, twist, or camber be shaped to produce a loading that sheds vortices with large cores (e.g., refs. 20, 51, 52, 55, and 56). Many of these span loadings had the characteristics that they tapered gradually to zero at the wing tips from an increased centerline loading. The properties of these loadings is illustrated by considering a so-called tailored loading (ref. 20) that produces a vortex sheet which rotates as a unit rather than rolling up from its edges (fig. 13). In this particular case, the velocity distribution in the wake was specified and the corresponding strengths of the vortex sheet and of the span loading were then found. When the vortex structure was compared with that for elliptic loading, it was found that the higher centerline lift required to maintain a given lift on the generator leads to higher rolling moments when the span of .the follower wing is more than about 0.2 of the span of the generating wing. This result is apparent in figure 14 when the circulation in the two vortices is compared for various span followers using equation (9) for the rolling moment.

These results and the guidelines developed in the previous subsection suggest that a span loading designed only on the basis of large vortex cores is not the proper direction for wake alleviation because these wings require higher centerline loadings. The corresponding decrease in b'_g/b_g associated with these loadings also suggests that a direct span loading — vortexcore design is not a good direction to proceed and that another approach should be tried.

Sawtooth Span Loadings for Vortex Dispersion

A second vortex-wake configuration studied theoretically in reference 20 was designed to translate downward as a unit (indicated schematically in fig. 15). This wake consisted not of a continuous vortex sheet but of a number of discrete vortices. The two-dimensional time-dependent theory for discrete vortices predicted that the vortex strengths required for such motion

alternate in sign across the span so that the span loading has a stepped or sawtooth shape as illustrated in figure 15. When the time-dependent method discussed previously is used to predict the shape of the wake, it is found to remain flat because all the individual vortices move downward at the same velocity. If, however, a disturbance is given to one of the vortices, the specified uniform motion breaks down and the vortices form pairs that make large excursions across the wake (as shown in fig. 16(a)). Hence, although the shape of the sawtooth loading fluctuates about elliptic loading, the vortices in the wake do not revolve about the edge or tip vortices in the way that they do for elliptic loading (fig. 16(b)). If a similar disturbance is given to the vortices shed by elliptic loading, the general shape of the wake is not altered, although the positions of some of the vortices change slightly.

The numerical result shown in figure 16(a) suggests that wakes with multiple vortex pairs can be designed *so* that they are unstable to disturbances, and convection of vorticity across the wake can be considerably enhanced by the resulting excursions of the vortex pairs. These theoretical results do not indicate whether the various pairs of vortices merge or link with one another to form a dispersed wake with low velocities, or if the vortices remain discrete with high core velocities. Insight into the characteristics of wakes shed by sawtooth loadings was obtained by flow-field observations made on two experimental wings configured to approximate sawtooth loading. The first wing was swept and equipped with seven flap segments per side (refs. 53 and 55). When these segments were deflected alternately up and down across the span, the loading is predicted by vortex-lattice theory to be as shown in figure 17. Tests by Ciffone and Orloff (ref. 55) in a water tow tank showed that the vortices shed by this wing did undergo large excursions in the wake and that various pairs linked in the way described by Scorer (ref. 45 and 46), Crow (ref. 37), and MacCready (ref. 2, p. 289). But when the various excursions and linking were completed, a vortex pair still remained in the wake. These preliminary results indicate that generation of multiple vortex pairs will bring about large vortex excursions that lead to linking, but additional criteria are needed to achieve adequate diffusion of the wake vorticity.

A second wing on which vortex wake alleviation was attempted by span-load modification was that of the Boeing *747* subsonic transport (refs. 80 and **83).** The wing has inboard and outboard flaps (fig. 18) that can be deflected separately *so* that the loading can be enhanced inboard or outboard within the limits indicated in figure 19. If the inboard flaps are deflected their full amount (30° setting), the span loading has a large hump inboard resembling a combination of tailored and sawtooth span loading. Although that loading produces three vortex pairs in the near-field rollup region, the two flap vortices combine, *so* that only two vortices per side persist into the far-field region. Far downstream, these two vortices of the same sign merge into a single diffuse vortex illustrated in figure 20. Tests in a water tow tank and in a wind tunnel indicate that the rolling moment imposed on a following aircraft by the wake of this configuration would be less than half that posed by the wake of the landing configuration at the same lift coef-ficient. Furthermore, this reduced value was below the roll-control capability of a LearJet aircraft which could be used to probe the wake. Flight tests conducted with the Boeing *747,* the LearJet, and a *T-37* aircraft (ref. *80)* confirmed the predictions of the ground-based facilities when the landing gear was retracted. **It** was found, however, that if any of the landing gears were extended or if the aircraft were yawed, the hazard alleviation achieved with the unconventional flap settings was greatly reduced.

These test results indicate that it is possible to induce large vortex excursions and reduced swirling velocities in the wake if substantial oscil-lations occur in the span loading. A theoretical estimate of the magnitude required was obtained in reference 20 by trying various types of span-load fluctuations and calculating whether dispersion occurred. It was found that the wake had a chaotic character if the loading variations in the loading were 30 percent or more of the maximum and if their spanwise sizes were about the same. The two-dimensional, time-dependent theory predicted that the multiple vortices shed into the wake would then undergo large excursions. Guidelines for whether the several vortex pairs will combine into a single pair in the far field by either a cutoff and linking process, or by a convective merging process, or neither are discussed in the next two subsections.

Before leaving this discussion, note that the vortex wakes of sawtooth loading will generally dissipate more rapidly than those of elliptic–like loadings for two reasons. First, each vortex pair in the wake is more closely spaced. Therefore, since the decay distance for a vortex pair depends on the distance between them (or on their effective span), the actual distance to a given dissipation (as given in figs. 8 and 9) would be decreased by the span ratio. Secondly, the theoretical analysis of Bilanin and Widnall (ref. 91) indicates that the sinusoidal instability is intensified by decreased spacing of vortices as the second power of span. It is not surprising then that the wakes produced by wings with multiple spanwise flap segments are often observed to dissipate more rapidly and to be less hazardous than wakes produced by wings with only one flap or none.

Self–Induced Vortex Excursions

The vortex pair behind aircraft flying at high altitudes is often observed (e.g., refs. 2, *37, 45, 46, 47,* and *48)* to undergo periodic, anti-symmetrical distortions that increase in amplitude until the vortices either appear to burst at the sharp bends or to link to form a series of loops. The linking process in such a vortex–vortex interaction occurs rapidly when the two equal and opposite vortices in the pair approach each other closely enough that the filaments appear to break in the flight direction and reconnect or link across the wake to form irregularly shaped loops that then disperse and decay. A comparison of the hazard posed by the vortex loops with that posed by the original parallel vortices needs to be made to determine whether a chance encounter with an axial segment of a loop is just as hazardous and whether flight across a segment of the vortex loop would cause unacceptable accelerations or air loads. Whether the loop stage of the wake is more or less hazardous than the original parallel–vortex stage is uncertain, but it seems apparent that the formation of loops enhances the decay and dispersion of the circulation in the wake.

A stability analysis by Crow (ref. *37)* showed that, once started, the wave growth results from the self–induced velocity field of the vortex pair with a preferred wavelength about 8.6 times the distance between the

32

vortices.   Other analyses (e.g., ref. 2) extended the analysis to include the effect of core size and axial velocities.   A numerical calculation using three–dimensional vortex filaments for the vortex pair has also been made by Hackett and Theisen (ref. 2 or 38) of the time history of the development of a periodic loop.

These research results demonstrate that antisymmetric, periodic, or sinusoidal disturbances on a vortex pair will lead to large self–induced excursions.   The mechanism by which the two vortices break from their original streamwise filament and link across to the other vortex in the pair has not been analyzed nor has the decay of the loops been treated adequately.   Added data are also needed on the effect of variables such as core size, axial velocity in the core, vortex strength, etc., when linking or bursting of the vortex filaments occurs.

The self–induced or sinusoidal instability for a single vortex pair has not proven to be a viable solution to the wake–vortex alleviation problem for several reasons.   First, the beginning of wave growth requires a disturbance from the atmosphere or from some periodic lift modification on the generating aircraft.   Introduction of a periodic span–load variation on the generating wing was shown by Bilanin and Widnall (ref. 91) to be an effective way to initiate growing waves that led to bursting when the curves in the vortex filaments reached a small radius of curvature.   Implementation of such a scheme on a full–sized aircraft would be difficult, however.   A second and more serious drawback is that the waves grow slowly and often become highly sinuous without bursting, linking, or appearing to decay.   Lastly, the large vortex cores produced by aircraft in the landing and takeoff configurations do not seem to be conducive to wave growth.

A new approach to stimulation or initiation of self–induced or vortex–vortex instabilities that led to large vortex excursions was suggested by the numerical analysis of wakes produced by the so–called sawtooth loadings studied in reference 20.   It was found that a wake with multiple vortex pairs about equally spaced across the span of the generating wing and of about the same magnitude but alternating in sign would undergo large excursions without being stimulated.   These self–induced excursions are not periodic, but are

often of the order of the span of the wing when the wake consists of vortices comparable in magnitude and alternating in sign.

As previously discussed, an experimental demonstration of the effectiveness of sawtooth loading for producing large vortex excursions was first made by Ciffone and Orloff (ref. 55) in a water tow tank. The wing was equipped with seven flap segments deflected alternately upward and downward by 15° to produce seven vortex pairs. A theoretical estimate of the span loading (fig. 17) indicates that the strengths of the vortices do alternate in sign and are about the same within a factor of 2. In the experiment, large vortex motions and linking occurred, but when the activity died down, a single residue vortex pair remained. Further theoretical and experimental studies are needed to arrange and match the vortex pairs to more completely disperse the wake so that the remaining velocities are tolerable and to possibly optimize the loading, Although the experiment was not completely successful, **it** did demonstrate that self-induced and rapid growth of vortex motions can be produced with sawtooth-type loadings. Another result found from the experiment was that **it** showed that linking could occur between opposite but not necessarily equal vortices. Such a partial linking process forms a series of vortex loops connected by vortex filaments. Convection of vorticity by the stronger vortex probably then causes the two vortices to completely merge by a process similar to that discussed in the next subsection (illustrated in fig. 21). An example of such a linking between an unequal vortex pair was observed in some flight experiments of Barber and will be presented by Corsiglia and Dunham in a paper to follow later in this conference. The interaction of the two opposite but unequal vortices from the flap has also been simulated numerically by Leonard (private communication) at ARC. These results indicate therefore that the multiple vortex pairs shed by sawtooth loading may provide a way to initiate the large vortex excursions and linking needed for alleviation. Various aspects of the dispersion and decay mechanisms need to be better defined and understood to make the method effective and to minimize penalties associated with these loadings and their implementation.

Convective Merging of Vortex Cores

The blending or merging of the several vortices shed by flap edges, pylons, horizontal tail, and the wing tip into a single vortex is a common and well-known occurrence.   The merging of two or more vortex cores (i.e., vortical regions) has also been studied theoretically from an inviscid point of view (e.g., refs. 92–97) and with a second-order turbulence theory (ref. 7).   Some results are now presented of a current study by the author that extends previous investigations by finding some circumstances under which two-dimensional inviscid vortex cores will or will not merge convectively.

Convective merging of the cores of two Rankine vortices is illustrated in figure 21.   The initial distribution of circulation is made approximately uniform over the circular regions of the cores by putting point vortices of the same strength on three circles at uniform intervals.   Since they each approximate Rankine cores, the maximum vortex velocity occurs at the outer ring.   The inner rings rotate more slowly so that the cores, when isolated, rotate as a solid body.   However, as shown in figure 21, when the two cores of the same sign and magnitude are placed in proximity but not touching, their mutual induction causes their shape to become distorted so that the two vortical regions reform into a single'region.

A slightly greater separation between the cores results in the vortices becoming only slightly elongated but not merging (fig. 22).   A series of such calculations was then used to determine a boundary between merging and nonmerging cases (fig. 23); that is, a combination of spacing and relative vortex strengths on the merging side of the curves do form a single vortical region from the original two circular regions.   In these cases, merger was assumed to have occurred whether one or both of the cores was reshaped in the process.   Note that merging occurs for vortices of opposite sign only when their relative strengths differ by a factor of about 5.

When a core structure other than Rankine is used, the merging process becomes more restrictive because the cores become effectively smaller relative to their spacing.   The boundaries for two other radial variations of circulation are also presented in figure 23 as dashed curves to show how the merging

region shrinks for more concentrated vortex cores. Since the vortex structures shed by flaps and wing tips are usually more concentrated than that for Rankine cores, and since merging requires a given maximum spacing, merging of two given vortices will be delayed until turbulence and viscosity diffuse the circulation to the degree needed for the convective redistribution to occur. The time-dependent calculations also showed that if convective merging is going to occur, it does so rapidly. Otherwise, the core shapes oscillate about their original circular shape.

Previous theoretical calculations indicate that the structure of a vortex pair consisting of two equal and opposite vortices, whether inviscid or including turbulence, will change very slowly with time (e.g., ref. 2, p. 413 ff; refs. 7 and 60). When the wake contains two or more pairs of vortices, the spacing between the vortices can change so that convective merging that would not occur at the outset does occur later. Another convenient set of guidelines is the vortex domain plots such as those prepared by Donaldson and Bilanin (fig. 2.2 of ref. 7). The boundaries shown for point vortices eliminate vortex combinations that will probably not be matched for convective merging or will not stay near one another long enough to merge. The number of remaining possibilities is still large and specific situations must be analyzed before the development of satisfactory guidelines has been completed.

CONCLUDING REMARKS

Inviscid modeling of lift-generated wakes has provided insight into the structure of the vortices and into means whereby wake velocities can be reduced or minimized. The available theories yield fairly good estimates for the wake-vortex structure (but not the axial flow) produced by the generating aircraft and for the wake dynamics in the so-called rollup and plateau regions. Satisfactory results are also obtained with inviscid theories for the loads induced by the wake on an aircraft as it enters along a near-axial flight path. As more comparisons are made with experiment, it may, however, be found necessary to include unsteady effects and better estimates of the lift curve. Some aspects of self-induced or vortex-vortex instabilities are

approximated by inviscid theories, but analyses and experiments currently
in progress may indicate that improved methods are needed.

The survey of alleviation schemes presented here indicates that more
complete theories are needed to aid the understanding of and to guide the
design of lifting systems that shed wakes which dissipate rapidly. The area
of greatest need is for methods that better represent continuous distributions
of vorticity so that flow processes such as vortex merging and linking can
be more accurately modeled. The most direct approach is probably through
numerical analysis of the flow field by a finite–difference scheme, Analyti-
cal approaches should, however, not be ruled out because well–defined guide–
lines can often be developed in this way if that portion of the flow field
which is of interest is properly approximated. If a numerical scheme is
developed, it should be easy to use and should not require substantial amounts
of computer time, because a large number of variables and a wide range of
conditions must be systematically considered to find those that provide
alleviation and those that will be optimum for various aircraft.

One approach presented here for wake–vortex alleviation suggests that
the span loading chosen should shed several vortex pairs of both signs so
that the vortices combine quickly to form a single pair low in strength and
widely spaced. A way to achieve this is to design the span loading so that
the centerline circulation is much lower than the maximum bound circulation
on the wing. The vortices must then be spaced and have such magnitudes that
they combine by convective merging and linking or both to form a single pair
not too far downstream which is relatively weak and with a large separation.
It may also be possible to arrange the loading *so* that this final pair is
also dispersed by linking. Indications from inviscid theory and from some
experiments are that a sawtooth–type loading that sheds multiple vortex pairs
of both signs may provide or have built into it the self–induced vortex
excursions needed to implement the linking process and the dispersion of
vorticity. However, more guidelines and a better understanding of these
flow fields, of the linking process, and of the decay of the vortex loops
produced are needed to make sawtooth loading a viable alleviation scheme.

Preliminary results from a theoretical two-dimensional study of convective merging of vortical regions indicate that further results will adequately define the conditions when merging will occur. Briefly, convective merging appears to be an effective process for combining vortical regions of the same sign that are relatively close to one another, but it is not particularly powerful for alleviating wake velocities because vortices of opposite sign do not readily merge convectively.

Inviscid theories have played an important role in the wake-vortex research program. Results from these theories should not be taken as final nor should they be considered as too inaccurate to be valid. When the inviscid methods are used where applicable and when the results are properly interpreted, they can continue to be useful for preliminary screening of wake-vortex alleviation schemes.

REFERENCES

1. Bleviss, Z. O.: Theoretical Analysis of Light Plane Landing and Take-off Accidents Due to Encountering the Wakes of Large Airplanes. Rept. SM-18647, Douglas Aircraft Corp., Santa Monica Div., Dec. 1954.

2. Olsen, John H.; Goldberg, Arnold; and Rogers, Milton, eds.: Aircraft Wake Turbulence. Plenum Publishing Corp., Sept. 1970.

3. El-Ramly, Z.: Aircraft Trailing Vortices — a Survey of the Problem. Tech. Rept. ME/A 72-1, Carleton Univ., Ottawa, Canada, Nov. 1972.

4. Kurylowich, G.: Analyses Relating to Aircraft Vortical Wakes. AFFDL/FGC-TM-73-23, Feb. 1973.

5. Gessow, A.: Aircraft Wake Turbulence Minimization by Aerodynamic Means. 6th Conference on Aerospace and Aeronautical Meteorology, El Paso, Texas, Nov. 12-14, 1974.

6. Roberts, L.: On Wake Vortex Alleviation. NASA/University Conf. on Aeronautics — Theme: The Future of Aeronautics, Univ. of Kansas, Oct. 23-24, 1974.

7. Donaldson, C. du P.; and Bilanin, A. J.: Vortex Wakes of Conventional Aircraft. AGARDograph 204, May 1975.

8. Rossow, Vernon J.: Survey of Computational Methods for Lift–Generated Wakes. Aerodynamic Analyses Requiring Advanced Computers, Part II, NASA SP–347, 1975, pp. 897–923.

9. Analytic Methods in Aircraft Aerodynamics. A symposium held at Ames Research Center, Moffett Field, Calif., NASA SP–228, 1969.

10. Aerodynamic Interference. AGARD Conference Proceedings No. 71, AGARD–CP–71–71, 1971.

11. Ashley, H.; and Rodden, W.P.: Wing–Body Aerodynamic Interaction. Ann. Rev. Fluid Mech., vol. 4, 1972, pp. 431–472.

12. Aerodynamic Analyses Requiring Advanced Computers, Parts I and II, NASA SP–347, 1975.

13. Maskew, B.: Numerical Lifting Surface Methods for Calculating the Potential Flow about Wings and Wing–Bodies of Arbitrary Geometry. Ph.D. Thesis, Loughborough Univ. of Tech., Oct. 1972.

14. Maskew, Brian: A Subvortex Technique for the Close Approach to Discretized Vortex Sheet. NASA TM X–62,487, 1975.

15. Kandil, O. A.; Mook, D. T.; and Nayfeh, A. H.: Nonlinear Prediction of the Aerodynamic Loads on Lifting Surfaces. AIAA Paper 74–503, 1974.

16. Chigier, N. A.; and Corsiglia, V. R.: Tip Vortices — Velocity Distributions. NASA TM X–62,087, 1971.

17. Hough, G.: Remarks on Vortex–Lattice Methods. AIAA J. Aircraft, vol. 10, no. 5, May 1973, pp. 314–317.

18. Rosenhead, L.: The Formation of Vortices from a Surface of Discontinuity. Proc. Roy. Soc. (London); vol. A134, 1931, pp. 170–192.

19. Westwater, F. L.: The Rolling Up of the Surface of Discontinuity Behind an Aerofoil of Finite Span. Reports and Memoranda 1692, British A.R.C., 1935, pp. 116–131.

20. Rossow, V. J.: Theoretical Study of Lift–Generated Vortex Wakes Designed to Avoid Roll Up. AIAA J., vol. *13,* no. *4,* April *1975,* pp. *476–484.*

21. Spreiter, J. R.; and Sacks, A. H.: The Rolling–Up of the Trailing Vortex Sheet and Its Effect on the Downwash Behind Wings. J. Aeronaut. Sci., vol. *18,* no. **1,** Jan. *1951,* pp. *21–32.*

22. Hama, F. R.; and Burke, E. R.: On the Rolling–Up of a Vortex Sheet. Tech. Note BN–220, AFOSR–TN *60–1069,* Univ. of Maryland, *1960.*

23. Takami, H.: A Numerical Experiment with Discrete–Vortex Approximation, with Reference to the Rolling Up of a Vortex Sheet. Sudaer 202 (AFOSR 64–1536), Sept. *1964.*

24. Moore, D. W.: The Discrete Vortex Approximation of a Vortex Sheet. Rept. *AFOSR–1084–69,* Calif. Inst. of Tech., *1971.*

25. Chorin, A. J.; and Bernard, P. S.: Discretization of a Vortex Sheet, with an Example of Roll–Up. College of Engineering Rept. *FM–72–5,* Univ. of California, Berkeley, Nov. *1972.*

26. Kuwahara, K.; and Takami, H.: Numerical Studies of Two–Dimensional Vortex Motion by a System of Point Vortices. J. Phys. Soc. Japan, vol. *34,* no. **1,** Jan. *1973,* pp. *247–253.*

27. Moore, D. W.: A Numerical Study of the Roll–Up of a Finite Vortex Sheet. J. Fluid Mech., vol. *63,* pt. 2, *1974,* pp. *225–235.*

28. Lin, C. C.: On the Motion of Vortices in Two Dimensions. No. *5,* Applied Mathematics Series, The Univ. of Toronto Press, Toronto, Canada, *1943.*

29. Betz, A.: Verhalten von Wirbelsystemen. Z.A.M.M., Bd. XII, Nr. *3, 1932,* pp. *164–174* (available as NACA TM *713).*

30. Rossow, V. J.: On the Inviscid Rolled–up Structure of Lift Generated Vortices. AIAA J. Aircraft, vol. 10, no. **11,** Nov. *1973,* pp. *647–650.*

31. Brashears, M. R.; Hallock, J. N.; and Logan, N. A.: Analysis of Predicted Aircraft Wake Vortex Transport and Comparison with Experiment, AIAA Paper *74–506, 1974* (to be published in Journal of Aircraft).

32. Hallock, J. N.; and Goldstone, L.: US/UK Vortex Monitoring Program at Heathrow Airport, AGARD Guidance and Control Panel 20th Symposium on Plans and Developments for Air Traffic Systems, Paper 24, 1975.

33. Hallock, J. N.; Wood, W. D.; and Spitzer, E. A.: The Motion of Wake Vortices in the Terminal Environment, AIAA/AMS Sixth Conference on Aerospace and Aeronautical Meteorology, Preprint Volume, 1974, pp. 393–398.

34. Brashears, M. R.; and Hallock, J. N.: Aircraft Wake Vortex Transport Model, J. Aircraft, vol. 11, no. 5, 1974, pp. 265–272.

35. Brashears, M. R.; and Hallock, J. N.: A Predictive Model of Wake Vortex Transport, AIAA/AMS Sixth Conference on Aerospace and Aeronautical Meteorology, Preprint Volume, 1974, pp. 387–392.

36. Brown, C. E.: Pressure Field of a Vortex Wake in Ground Effect. AIAA J. Aircraft, vol. 12, no. 2, Feb. 1975, pp. 120–121.

37. Crow, S. C.: Stability Theory for a Pair of Trailing Vortices. AIAA J., vol. 8, no. 12, Dec. 1970, pp. 2172–2179.

38. Hackett, J. F.; and Theisen, J. G.: Vortex Wake Development and Aircraft Dynamics, Aircraft Wake Turbulence and Its Detection, edited by J. H. Olsen et al., Plenum Press, New York, 1971, pp. 243–263.

39. Widnall, S. E.; Bliss, D.; and Zalay, A.: Theoretical and Experimental Study of the Stability of a Vortex Pair, Aircraft Wake Turbulence and Its Detection, edited by J. H. Olsen et al., Plenum Press, New York, 1971, pp. 305–338.

40. Saffman, P. G.: The Motion of a Vortex Pair in a Stratified Atmosphere, Studies in App. Math.; vol. LI, 1972, pp. 107–119.

41. Hama, F. R.: Progressive Deformation of a Carved Vortex Filament by its *Own* Induction, Phys. Fluids, vol. 5, no. 10, Oct. 1962, pp. 1156–1162.

42. Moore, D. W.; and Saffman, P. G.: The Motion of a Vortex Filament with Axial Flow. Phil. Trans. Roy. Soc., series A, vol. 272, 1972, p. 403.

43. Leonard, A.:   Simulation of Unsteady Three–Dimensional Separated Flows with Interacting Vortex Filaments.   Aerodynamic Analyses Requiring Advanced Computers, Part II, NASA *SP–347, 1975,* pp. *925–937.*

44. Moore, D. W.;   and Saffman, P. G.:   A Note on the Stability of a Vortex Ring of Small Cross Section.   Proc. Roy. Soc. London, series A, vol. *338, 1974,* pp. *535–537.*

45. Scorer, R. S.:   Natural Aerodynamics, Pergamon Press, New York, *1958.*

46. Scorer, R. S.; and Davenport, L. J.:   Contrails and Aircraft Downwash, J. Fluid Mech., vol. *43, 1970,* pp. 451–464.

47. Harvey, J. K.; and Fackrell, J. E.:   Observation of a Mechanism Causing a Trailing Contrail Vortex to Break Up, Aero Rept. *70–08,* Imperial College, London, *1970.*

48. Tombach, I.:   Observations of Atmospheric Effects of Vortex Wake Behavior.   AIAA J. Aircraft, vol. 10, no. 11, Nov. *1973,* pp. *641–647.*

49. Donaldson, Coleman du P.:   A Brief Review of the Aircraft Trailing Vortex Problem, A.R.A.P.   Rept. *155,* May *1971.*

50. Donaldson, C. du P.; Snedeker, R. S.; and Sullivan, R. D.:   Calculation of Aircraft Wake Velocity Profiles and Comparison with Experimental Measurements.   AIAA J. vol. 11, no. *9,* Sept. *1974,* pp. 547–555.

51. Mason, H. W.; and Marchman, J. F., III: The Farfield Structure of Aircraft Wake Turbulence.   AIAA Paper *72–40, 1972.*

52. Brown, C. E.:   Aerodynamics of Wake Vortices.   AIAA J., vol. 11, no. *4,* April *1973,* pp. *531–536.*

53. Rossow, V. J.; Corsiglia, V. R.; Schwind, R. G.; Frick, J. K. D.; and Lemmer, O. J.:   Velocity and Rolling Moment Measurements in the Wake of a Swept Wing Model in the *40–* by 80–Foot Wind Tunnel.   NASA TM *X–62,414, 1975.*

54. Bilanin, A. J.; and Donaldson, C. du P.:   Estimation of Velocities and Roll–Up in Aircraft Vortex Wakes.   AIAA J. Aircraft, vol. *12,* no. *7,* July *1975,* pp. *578–585.*

55. Ciffone, D. L.; and Orloff, K. L.: Far–Field Wake–Vortex Characteristics of Wings. AIAA J. Aircraft, vol. 12, no. 5, May 1975, pp. 464–470.

56. Rossow, V. J.: Prediction of Span Loading from Measured Wake–Vortex Structure — An Inverse Betz Method. AIAA J. Aircraft, vol. 12, no. 7, July 1975, pp. 626–628.

57. Donaldson, C. du P.: Calculation of Turbulent Shear Flows for Atmospheric and Vortex Motions. AIAA J., vol. 10, 1972, pp. 4-12.

58. Iversen, J. D.: Correlation of Turbulent Trailing Vortex Decay Data. AIAA J. Aircraft (to be published).

59. Ciffone, D. L.: Correlation for Estimating Vortex Rotational Velocity Downstream Dependence. AIAA J. Aircraft, vol. 11, no. 11, Nov. 1974, pp. 716-717.

60. Iversen, J. D.: Inviscid to Turbulent Transition of Trailing Vortices. Paper ISU-ERI-Ames-74241, Iowa State Univ., Engineering Research Inst., Nov. 1974.

61. Heaslet, M. A.; and Spreiter, J. R.: Reciprocity Relations in Aerodynamics, TN 2700, 1952, NACA.

62. Rose, R.; and Dee, F. W.: Aircraft Vortex Wakes and Their Effects on Aircraft, RAE Tech. Note Aero 2934, Dec. 1963.

63. McGowan, W. A.: Calculated Normal Load Factors on Light Airplanes Traversing the Trailing Vortices of Heavy Transport Airplanes, NASA TN D-829, March 1969.

64. McGowan, W. A.: Trailing Vortex Hazard. SAE Transactions, Rept. 68–220, vol. 77, 1968, pp. 740-753.

65. Wetmore, J. W.; and Reeder, J. P.: Aircraft Vortex Wakes in Relation to Terminal Operations. NASA TN D-1777, April 1963.

66. Miller, E. R., Jr.; and Brown, C. W.: An Experimental Study of Trailing Vortex Wakes Using a Large Towing Tank, Hydronautics, Inc., Laurel, Md., Aug. 1971.

67. Jones, W. P.; and Rao, B. M.: Airloads and Moments on an Aircraft Flying over a Pair of Inclined Trailing Vortices, Aircraft Wake Turbulence and Its Detection, Plenum Press, 1971.

68. Hackett, J. E.; and Theisen, J. G.: Vortex Wake Development and Aircraft Dynamics, Aircraft Wake Turbulence and Its Detection, edited by J. Olsen, A. Goldberg, and M. Rogers, Plenum Press, New York, 1971.

69. Corsiglia, V. R.; Jacobsen, R. A.; and Chigier, N.: An Experimental Investigation of Trailing Vortices Behind a Wing with a Vortex Dissipator, Aircraft Wake Turbulence and Its Detection, edited by J. Olsen, A. Goldberg, and M. Rogers, Plenum Press, New York, 1971.

70. Jones, W. P.: Vortex–Elliptic Wing Interaction. AIM J., vol. 10, no. 2, Feb. 1972, pp. 225–227.

71. Filotas, L. T.: Vortex Induced Wing Loads. AIM J., vol. 10, no. 7, July 1972, p. 971.

72. Andrews, William H.; Robinson, Glenn H.; and Larson, Richard R.: Exploratory Flight Investigation of Aircraft Response to the Wing Vortex Wake Generated by Jet Transport Aircraft, NASA TN D–6655, March 1972.

73. Wentz, W. R., Jr.: Evaluation of Several Vortex Dissipators by Wind Tunnel Measurements of Vortex–Induced Upset Loads. Aeronautical Rept. 72–3, Wichita State Univ., Sept. 1972.

74. Robinson, Glenn H.; and Larson, Richard R.: A Flight Evaluation of Methods for Predicting Vortex Wake Effects on Trailing Aircraft, NASA TN D–6904, Nov. 1972.

75. Harlan, Raymond B.; and Madden, Stephen J., Jr.: A Hazard Definition for Wake Turbulence Encounter During Terminal Area Operations, MIT–MSL–RE–81, Mar. 1973.

76. Banta, A. J.: Effects of Planform and Mass Injection on Rolling Moments Induced by Trailing Vortices. M. S. Thesis, Wichita State Univ., Dec. 1973.

77. Kirkman, K. L.; Brown, C. E.; and Goodman, A.: Evaluation of Effectiveness of Various Devices for Attenuation of Trailing Vortices Based on Model Test in a Large Towing Basin. NASA CR–2202, Dec. 1973.

78. Nelson, R. C.: The Response of Aircraft Encountering Aircraft Wake Turbulence. AFFDL TR 74–29, June 1974.

79. Nelson, R. C.; and McCormick, B. W.: The Dynamic Behavior of an Aircraft Encountering Aircraft Wake Turbulence. AIAA Paper 74–774, Aug. 1974.

80. Tymczyszyn, J.; and Barber, M. R.: A Review of Recent Wake Vortex Flight Tests. 18th Annual Symposium of Society of Experimental Test Pilots, Los Angeles, Calif., Sept. 26, 1974.

81. Hastings, E. C., Jr.; Shanks, R. E.; Champine, R. A.; and Copeland, W. L.: Preliminary Results of Flight Tests of Vortex Attenuating Splines. NASA TM X–71928, 1974.

82. Johnson, Walter A.; and Teper, Gary L.: Analysis of Vortex Wake Encounter Upsets, Systems Technology, Inc., Tech. Rept. 1025–2.

83. Corsiglia, V. R.; Rossow, V. J.; and Ciffone, D. L.: Experimental Study of the Effect of Span Loading on Aircraft Wakes. AIAA Paper 75–885, 1975 (see also NASA TM X–62,431, 1975).

84. Patterson, J. C., Jr.; and Flechner, S. G.: An Exploratory Wind-Tunnel Investigation of the Wake Effect of a Panel Tip-Mounted Fan-Jet Engine on the Lift-Induced Vortex, NASA TN D–5729.

85. Hastings, E. C., Jr.; Patterson, J. C., Jr.; Shanks, R. A.; Champine, R. A.; Copland, W. L.; and Young, D. C.: Development and Flight Test of Vortex Attenuating Splines, NASA TN D–8083, Sept. 1975.

86. Patterson, J. C., Jr.: Vortex Attenuation Obtained in the Langley Vortex Research Facility. AIAA J. Aircraft, vol. 12, no. 9, Sept. 1975, pp. 745–749.

87. Iverson, James D.; and Bernstein, Shmuel: Trailing Vortex Effects on Following Aircraft. AIAA J. Aircraft, vol. 11, no. 1, Jan. 1974, pp. 60–61.

88. Iverson, J. D.; and Bernstein, S.: Dynamic Simulation of an Aircraft Under the Effect of Vortex Wake Turbulence, Annales de l'Association pour le Calcul Analogique, vol. *14, 1972,* pp. *136-144.*

89. Jones, R. T.; and Cohen, D.: Aerodynamics of Wings at High Speeds. Aerodynamic Components of Aircraft at High Speeds, vol. VII, edited by A. F. Donovan and H. R. Lawrence, Princeton Univ. Press, *1957.*

90. Ciffone, Donald, L.: Vortex Interactions in Multiple Vortex Wakes Behind Aircraft. AIAA Paper *76-62, 1976.*

91. Bilanin, A. J.; and Widnall, S, E.: Aircraft Wake Dissipation by Sinusoidal Instability and Vortex Breakdown. AIAA Paper *73-107, 1973.*

92. Moore, D. W.; and Saffman, P. G.: Structure of a Line Vortex in an Imposed Strain. Aircraft Wake Turbulence and Its Detection, edited by J. H. Olsen et al., Plenum Press, New York, **1971,** pp. *339-354.*

93. Roberts, K. V.; and Christiansen, J. P.: Topics in Computational Fluid Mechanics. Computer Phys. Commun, Suppl., vol. *3,* Sept. *1972,* pp. *14-32.*

94. Christiansen, J. P.: Numerical Simulation of Hydrodynamics by the Method of Point Vortices. J. Computational Phys., vol. **13,** no. *3,* Nov. *1973,* pp. *363-379.*

95. Christiansen, J. P.; and Zabusky, N. J.: Instability, Coalescence and Fission of Finite-Area Vortex Structures. J. Fluid Mech., vol. *61,* pt. *2,* Nov. *6, 1973,* pp. *219-243.*

96. Winant, C. D.; and Browand, F. K.: Vortex Pairing: the Mechanism of Turbulent Mixing-Layer Growth at Moderate Reynolds Number. J. Fluid Mech., vol. *63,* pt. *2, 1974,* pp. 237-255.

97. Moore, D. W.; and Saffman, P. G.: The Density of Organized Vortices in a Turbulent Mixing Layer. J. Fluid Mech., vol. *69,* pt. *3, 1975,* pp. *465-473.*

TABLE I.- COMPARISON OF PREDICTED AND MEASURED ROLLING-MOMENT COEFFICIENTS (from ref. 53).

Configuration	α, deg	C_{L_g}	b_f/b_g	AR_f	Normalized rolling moment, C_{l_f}/C_{L_g}			
					Measured[a]	Strip theory		Vortex-lattice theory, Flat-wake approximation
						$C_{L_\alpha} = 2\pi$	Empirical C_{L_α}	
Flaps 0°	8	0.75	0.29	5.84	0.092	0.222	0.110	0.109
Flaps 0° plus spoiler	8	.70	---	---	.053	.184	.091	.085
Landing	6	.85	---	---	.081	.243	.120	.117
Landing plus spoiler	8	.86	---	---	.081	.163	.081	.071
Tailor[a]	10	.82	---	---	.105	.246	.122	.111
Flaps 0°	8	.75	.14	2.82	.099	.317	.101	.090
Flaps 0° plus spoiler	8	.70	---	---	.023	.154	.049	.038
Tailor[a]	10	.82	---	---	.074	.173	.055	.042
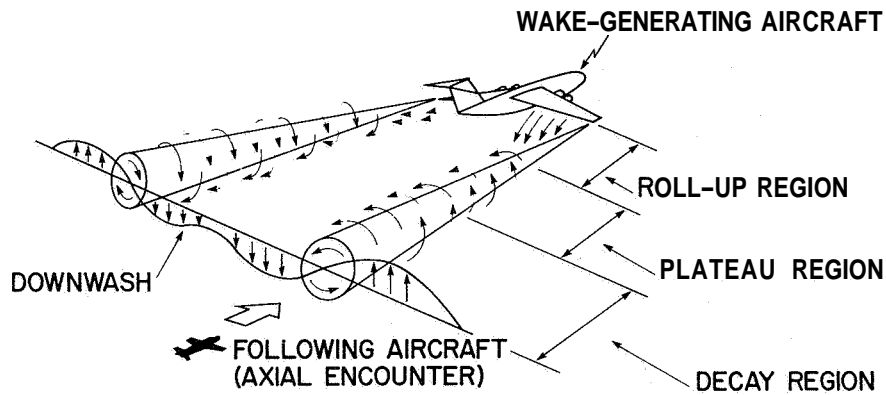
Figure 1.- Flow field produced by lift-generated vortices; distances not drawn to scale.
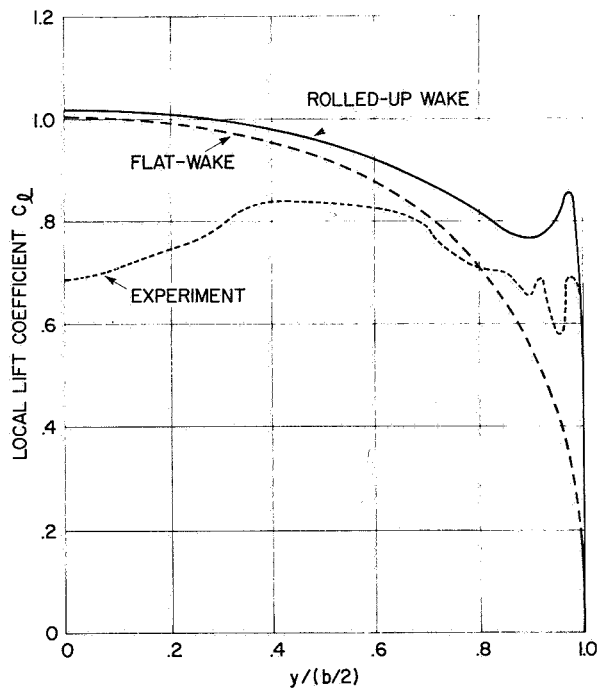
Figure 2.- Measured spanwise lift distribution on rectangular wing compared with loading predicted by vortex-lattice theory assuming that wake is flat and that near wake is rolling up; $a = 12°$. (From B. Maskew, private communication.)

48
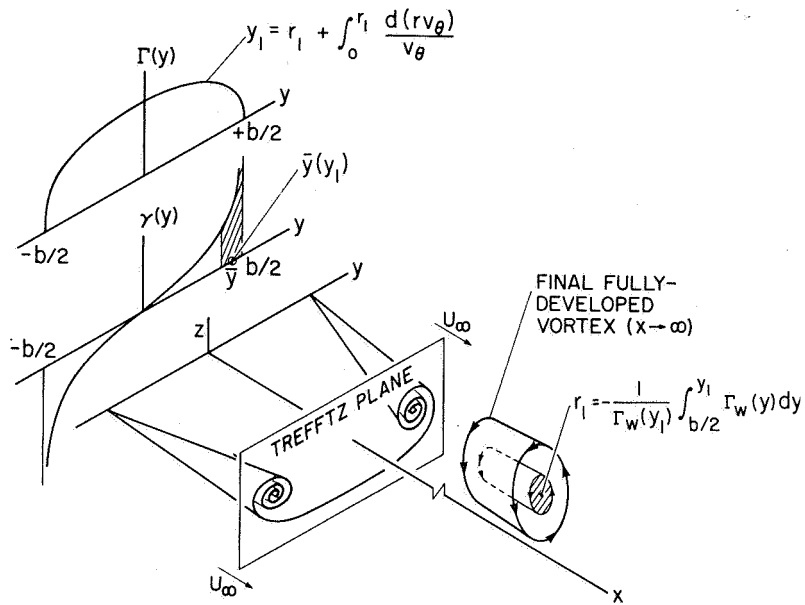
Figure 3.- Schematic diagram of wake rollup and relationships between span loading and vortex structure.
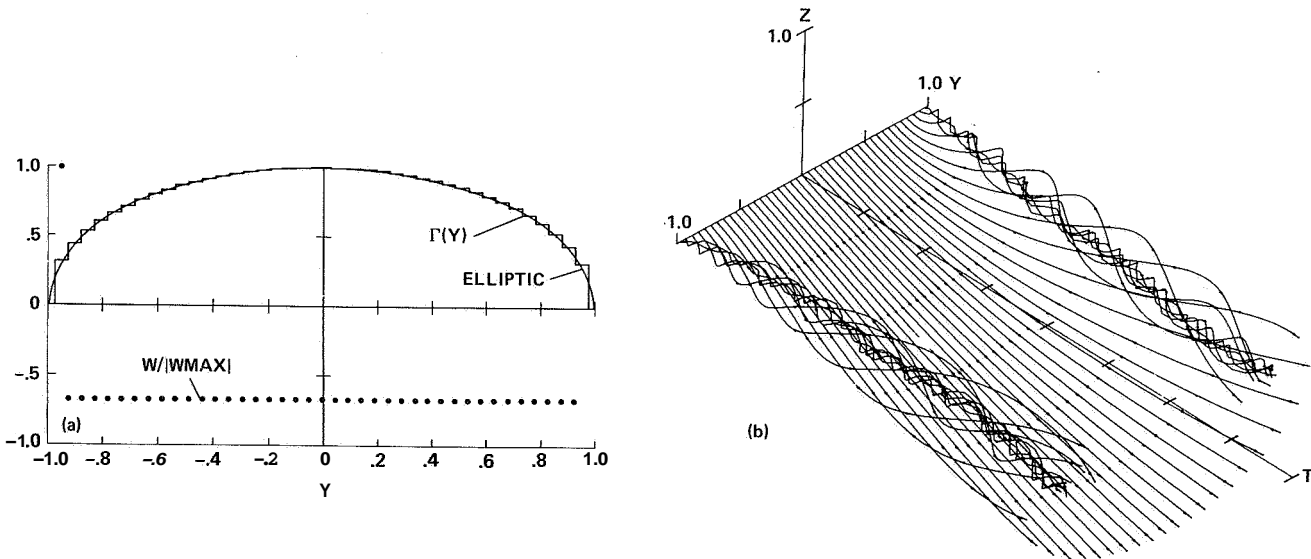
Figure 4.- Rollup of vortex wake shed by elliptic loading calculated by inviscid two-dimensional time-dependent approximation; W is dimensionless vertical velocity (from ref. 20).
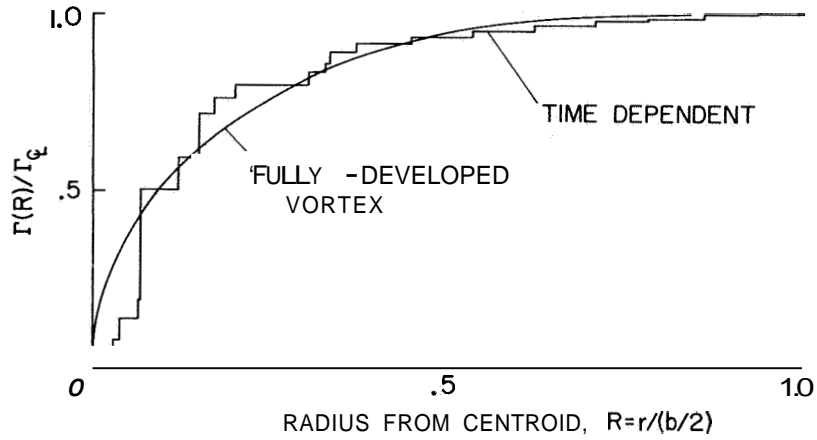
Figure 5.– Comparison of structure of vortex shed by elliptic loading as predicted by time–dependent method with that predicted by the Betz direct rollup theory; Γ_{C_L} is circulation on centerline (from ref. 20).
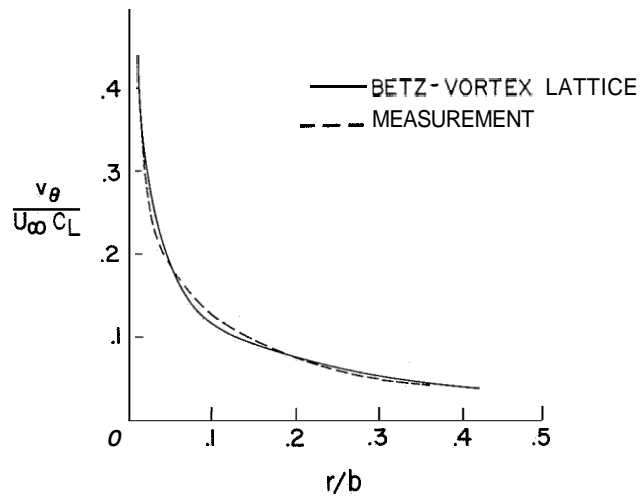
Figure 6.– Comparison of measured vortex structure with prediction made by the Betz rollup theory using span loading predicted by vortex–lattice theory for a swept wing that approximates CV–990 wing (from ref. 53).
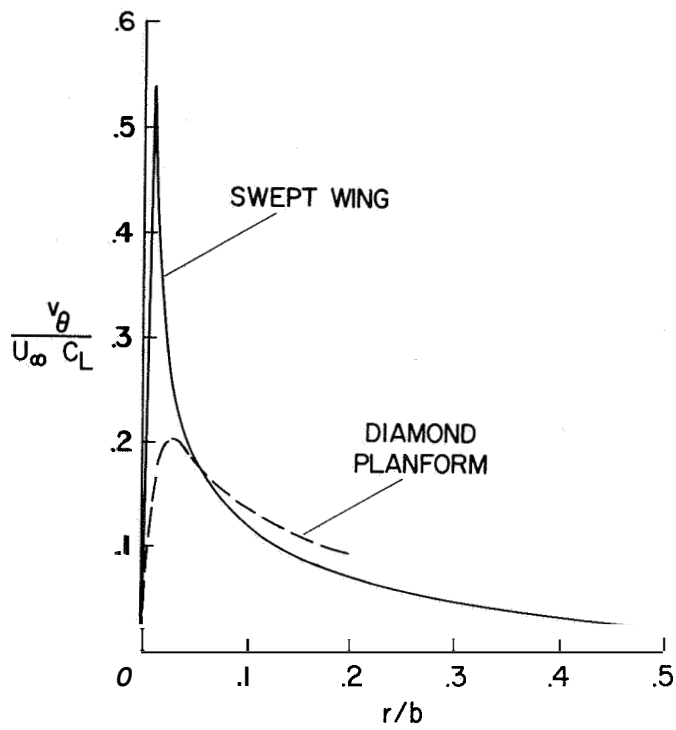
(a) Measured vortex velocity profiles (ref. *53*).
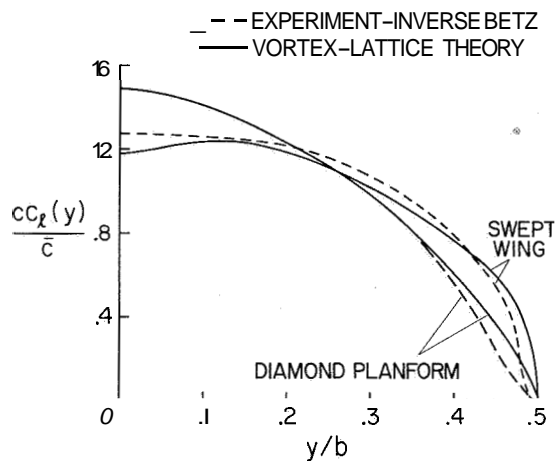
(b) Calculated span loadings.

Figure **7.**– Comparison of inverse rollup theory with vortex – lattice theory (from ref. 56).
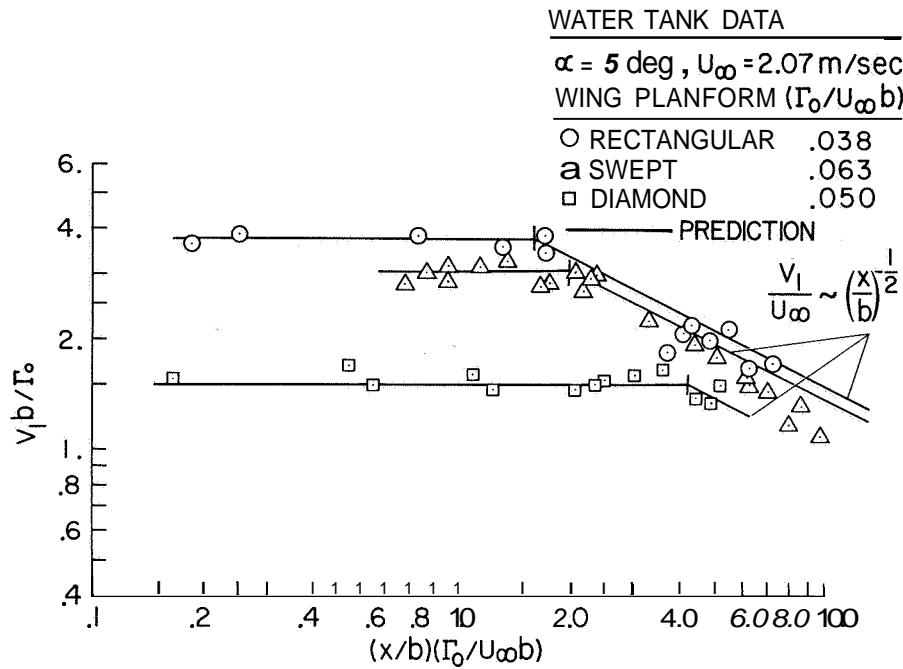
Figure 8.– Maximum circumferential velocity in vortices behind wings as measured in water tow tank (from Ciffone and Orloff, ref. 55).
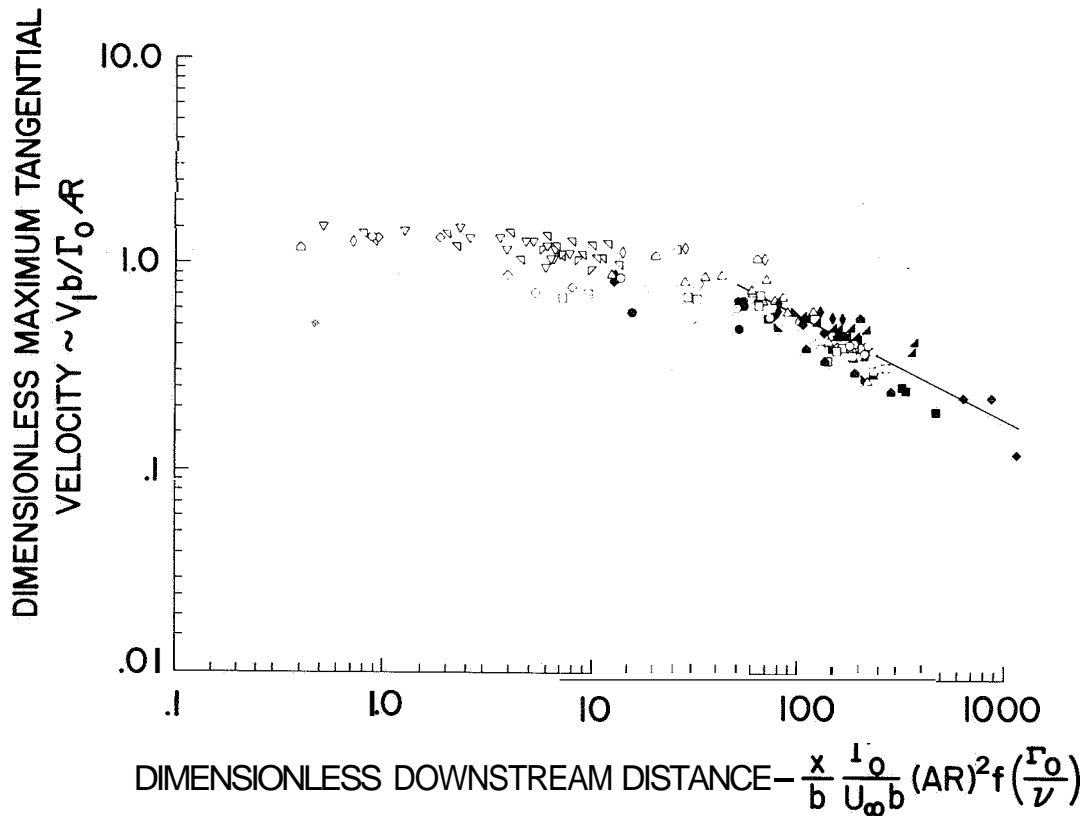
Figure 9.– Correlation of data from ground–based and flight experiments on maximum circumferential velocity in vortices shed by various conventional span loadings (from Iversen, ref. 58).
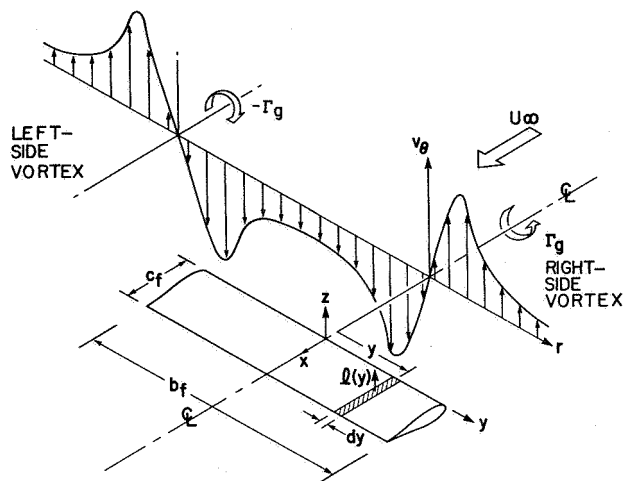
Figure 10.– Wake vortex pair impinging on a follower wing.
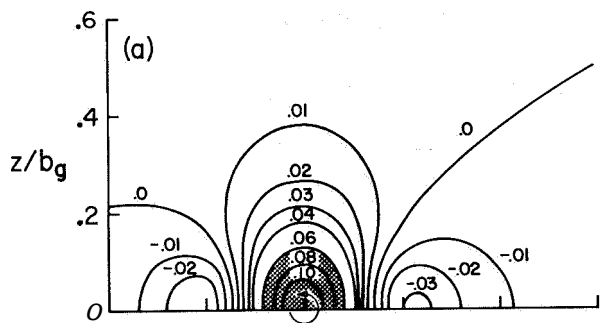
(a) Contours of equal rolling–moment parameter, C_{l_f}/C_{L_g}; $C_{l_f})_{max}/C_{Lg} = 0.122$.
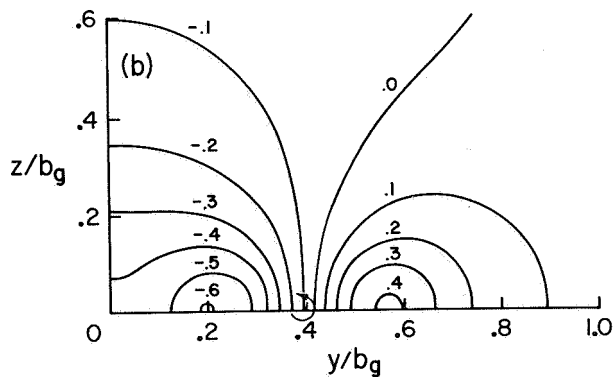
(b) Contours of equal lift parameter, C_{L_f}/C_{L_g}; $C_{L_f})_{max}/C_{L_g} = -0.88$.

Figure 11.– Rolling moment and lift induced on the follower wing by the wake of a swept wing; tailored loading, $b_f/b_g = 0.29$ (from ref. 53).

	α, deg	C_{L_T}	C_{D_i}	CONFIGURATION
—··—	14	1.08	0.061	CLEAN
——	29	1.09	0.103	LDG
— — —	29	0.90	0.810	MOD LDG
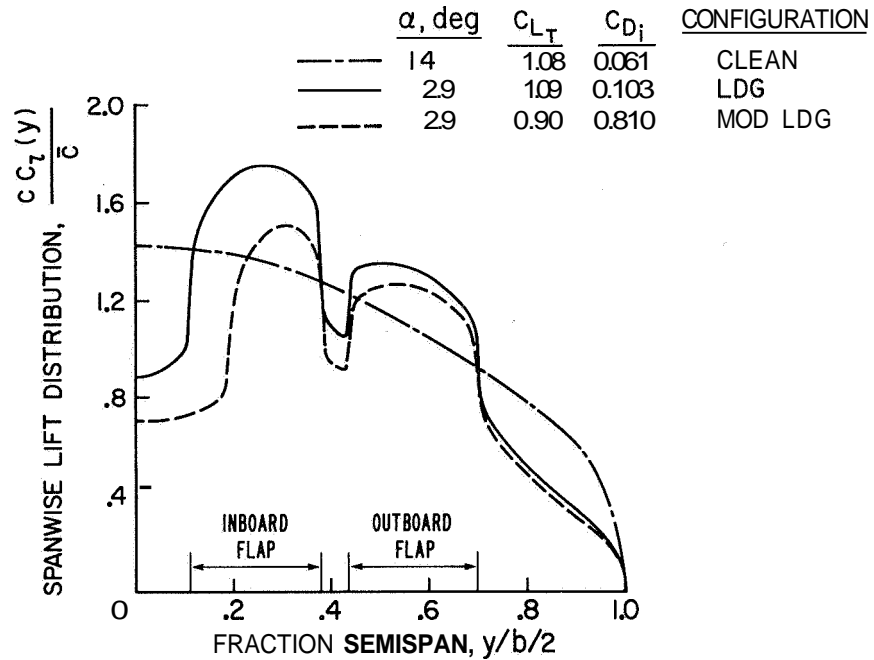
Figure 12.– Span loadings predicted by vortex–lattice theory for Boeing 747 wing without a fuselage (from Ciffone, ref. 90).
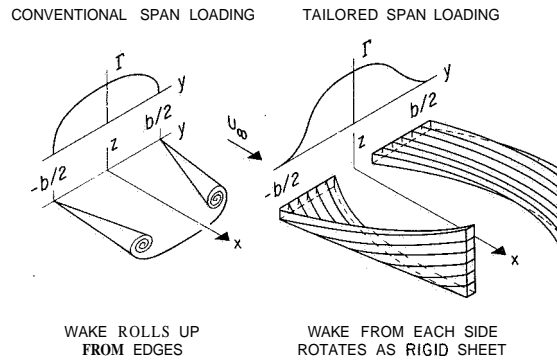
Figure 13.– Comparison of conventional wake with hypothetical wake designed to have parts that rotate as a unit without rolling up from its edges (from ref. 20).

54

3
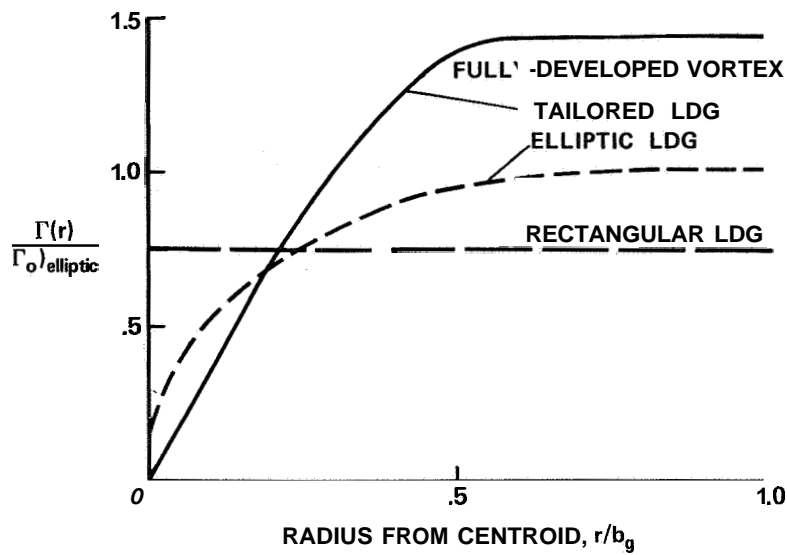
Figure 14.– Radial distribution of circulation in wake vortices shed by
.90 percent tailored loading as predicted by Betz' theory for fully
developed vortices.
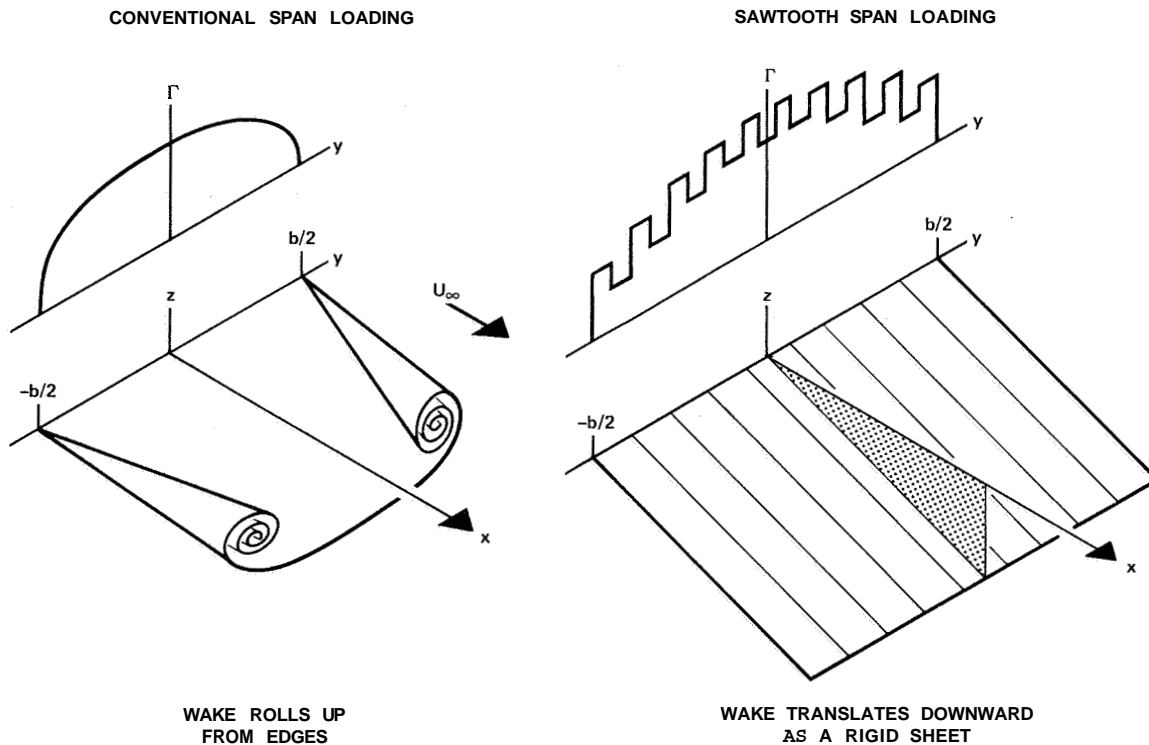
Figure 15.– Comparison of conventional wake with a hypothetical wake
designed to translate downward as a unit.

55
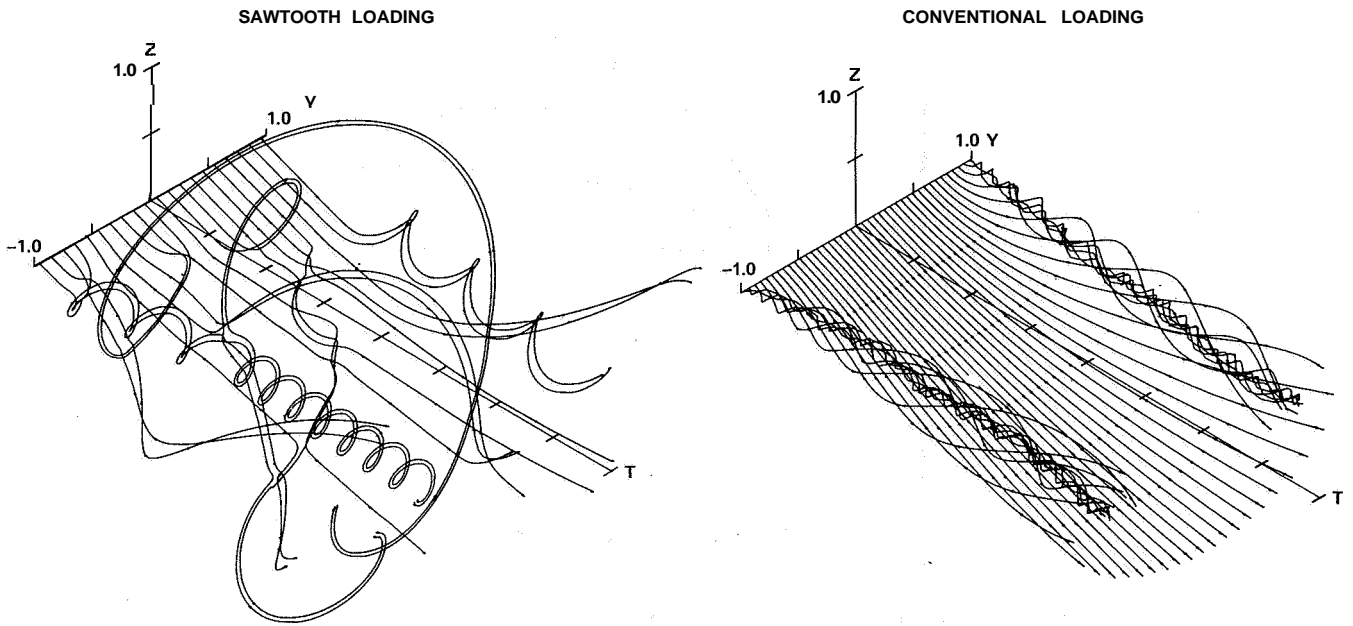
(a) Large–scale wake mixing.   (b) No wake mixing.

Figure 16.– Wake structure predicted by time–dependent vortex calculations for elliptic and sawtooth span loadings (from ref. 20).

SAWTOOTH LOADING ON CV990 WING
$C_L = 0.7$
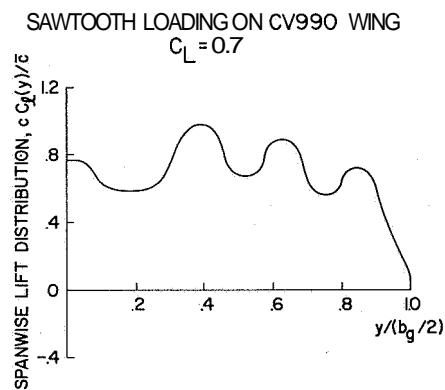
Figure 17.– Span loading predicted by vortex–lattice theory for swept wing with seven flap segments per side deflected alternately up and down 15°; $C_L = 0.7$ (from ref. 53).
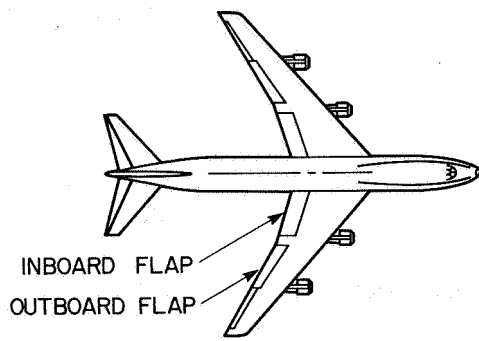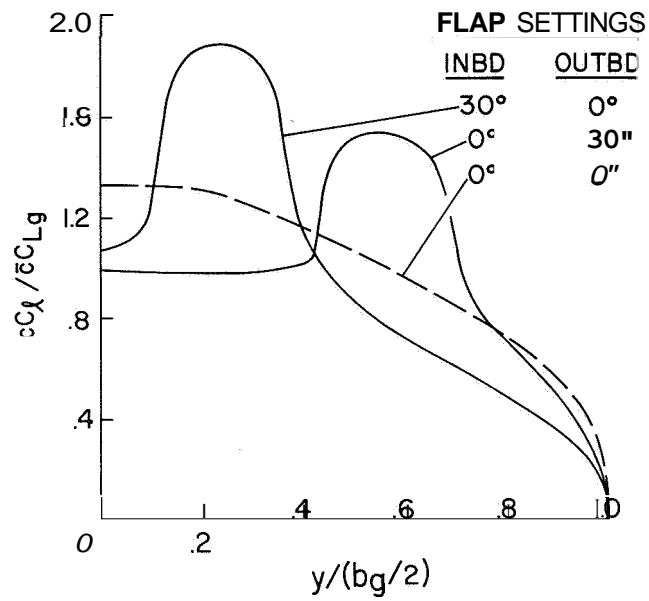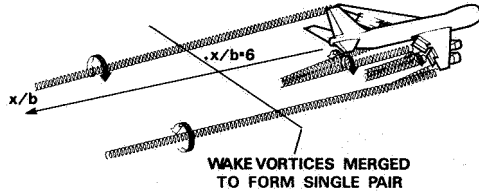
Figure 18.– Plan view of Boeing 747 subsonic transport.

Figure 19.– Span loadings calculated for Boeing 747 wing using vortex–lattice theory (from ref. 83).

CONVENTIONAL LANDING CONFIGURATION

x/b•6

x/b

WAKE VORTICES MERGED
TO FORM SINGLE PAIR

MODIFIED LANDING CONFIGURATION (LDG/0°)

FLAP INBOARD AND
OUTBOARD VORTICES MERGE

FLAP AND TIP VORTICES
MERGE (GEAR UP)

1.5

13

6

x/b
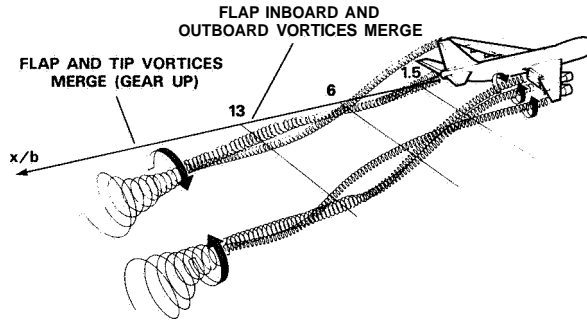
Fig. 20.- Comparison of two wakes of Boeing 747 (from ref. 83).

$$\Gamma_1 = \Gamma_2$$
$$d_s = 1.7\, d_c$$

Γ_2

Γ_1 T = 0

d_c

T = 1

d_s

VORTEX C.G. LOCATIONS

e.

T = 2

T = 3
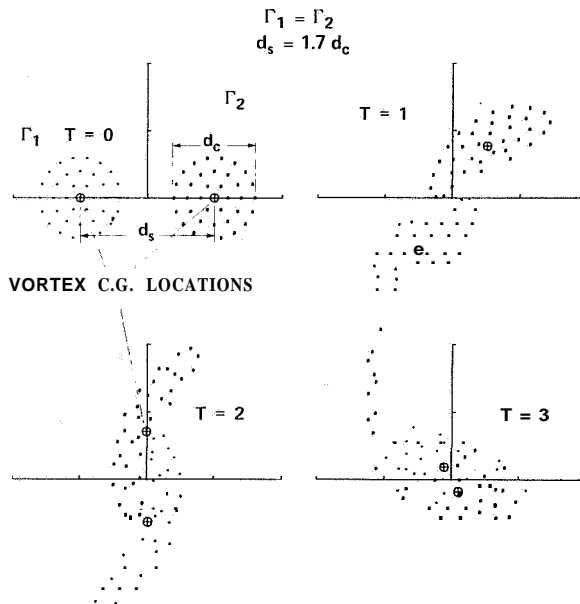
Fig. 21.- Merging sequence predicted numerically for two Rankine vortices of

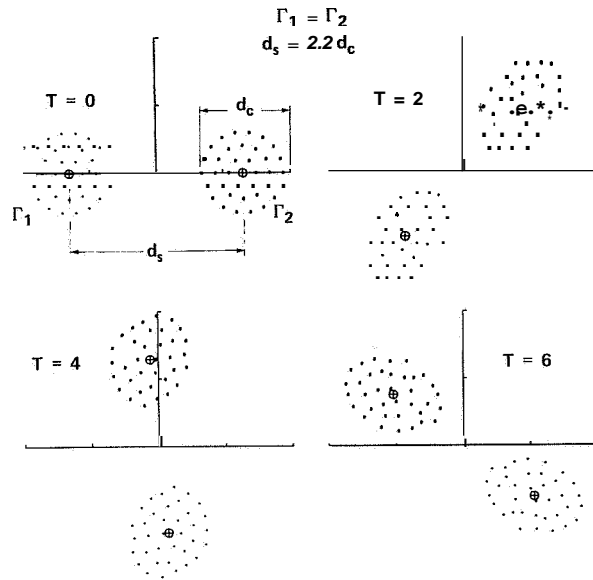equal strength, $\Gamma_1 = \Gamma_2$ and $d_s = 1.7 d_c$.

58

Figure 22.– Case where two Rankine vortex cores do not merge because spacing between them is too large; $d_s = 2.2d_c$, $\Gamma_1 = \Gamma_2$.
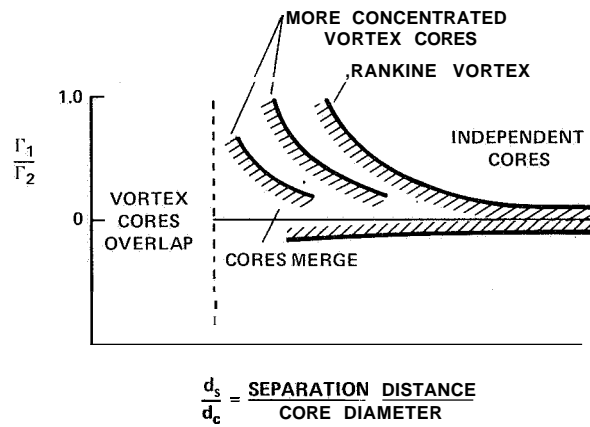

Figure 23.– Combinations of strength and spacing required for Rankine vortex cores to merge.